Investigation of a robust controller, based on the adaptive computed torque method

Groeneweg, E.J.

Award date:
1991

Investigation of a robust controller, based on the adaptive computed torque method

E.J. Groeneweg

WFW report 91.044

Professor: Dr.ir. J.J. Kok
Coach: Ir. A.G. de Jager

June 1991

Eindhoven University of Technology
Department of Mechanical Engineering
Division of Mechanical Engineering Fundamentals

Contents

Summary

Mechanical manipulators are controlled in order to make their end-effector track a desired trajectory. For this reason controllers are designed based on available information of the system dynamics. From this information a model is derived, which does not correspond exactly to the actual system. Due to measurement noise, unmodelled dynamics (i.e. dynamics, that are not accounted for in the control model) and unknown parameters, model errors always will occur. A controller, whose control behaviour isn't influenced too much by model errors, is called a robust controller.

Because only a few of the robust controllers, which are presented in literature, are used in practice, research has to be done about the feasibility of those controllers. In this report the feasibility of the controller, designed by R.Kelly [1], is investigated. This controller is reasonably robust and has a good tracking accuracy. It estimates the parameters on-line and therefore it is very useful, when parameters are unknown.

This report consist of three parts, where the following topics are discussed:

- Simulations of a controlled RT-robot, which is a rigid manipulator.
- Simulations of a controlled XY-table, which is a flexible manipulator.
- Experiments with the XY-table

A comparison is made between the controller of R.Kelly and the controller, proposed by Slotine-Li [2]. This is done in all three parts, mentioned above.
First simulations are done with the RT-robot, also when unmodelled dynamics are added. Secondly the performances are investigated, when simulating a controlled XY-table. Finally research is done into the influence of unmodelled dynamics of the actual XY-table.

There is not much difference between the controllers, when systems are controlled without centripetal- or Coriolis forces. An investigation should be done, where the controllers are used in such situations.

Notation

A,a	; scalar number
A	: matrix (capital *italic* characters)
a	: column (small *italic* characters)
a_i	: i-th term of column
a^T, A^T	: transposition of column or matrix
A^{-1}	: inverse of matrix
$\hat{a}$,$\hat{a}$	: estimate of scalar or column
a_d,a_d	: desired scalar or column
$\tilde{a}$	: a_d -a (tracking error)
$\dot{a}$	: first order derivative ($\frac{\partial a}{\partial t}$)
$\ddot{a}$	: second order derivative
I	: Unity matrix

Chapter 1:

Introduction

Industrial robots are controlled in order to make their end-effector track a desired trajectory. It is desirable to have full knowledge of the system. A controller using a model with full dynamics feedforward, would track the trajectory without tracking errors. In practice the model will never correspond exactly to the real system. Some of the following modelling errors will always occur:

- The *dynamic structure* of the model does not match the system. A mechanical manipulator is often considered stiff for example, while there exists a significant flexability.
- The *dynamic structure* of the model matches the system, but the *parameter-values* are not estimated right. These parameters contain physical properties and geometrical properties. Physical properties are mass, inertia gravitation and frition. Examples of geometrical properties are length and angle.
- The controller design is often based on a continuous time model. On-line control takes processing time, which causes tracking errors.

Taking in account these modelling errors, a controller using only full dynamics feedforward would make large tracking errors. A controller is robust, when model errors have little influence on the control behaviour.

In literature many robust controllers are proposed, but only a few are actually applied. To examine the practical application of existing controllers, the feasibility of a robust controller, proposed by R. Kelly [1], is investigated in this report. This controller is based on an adaptive *Computed-Torque* method. Also the performances of this controller and the controller suggested by Slotine and Li [2], and investigated by L. v. Gerwen [4], will be compared.

In chapter 2 the principles of both controllers are explained and discussed.

In chapter 3 the simulations of a controlled RT-robot are presented. First the mathematical discription of the robot is given. Secondly simulations with an exactly matching model, simulations with unmodelled dynamics and simulations with friction are presented.

In chapter 4 information about simulations with a controlled XY-table,which is a flexible manipulator, is given. In the first paragraph the reduced model for the controllers is given. In the second paragraph the control parameters are derived. Furthermore the results of the simulations are shown.

In chapter 5 results of the application of both controllers to the actual XY-table are given. To reduce the errors, which were the result of measurement noise and processing time, the velocities and positions were estimated with a Kalman observer, designed in paragraph 5.3. Experiments were done in two situations:

- without using the torsion spring, i.e. a rigid system
- when using the torsion spring, i.e. a flexible system

In both situations the controllers are compared.

In chapter 6 conclusions are drawn from the results, obtained in chapters 3, 4 and 5. Recommandations are given for further experiments, which will lead to a better understanding of the capabilities of both controllers.

Chapter 2:

Control strategy

In this chapter the control strategy of R.Kelly and that of Slotine-Li will be discussed.
In the following two paragraphs the mathematical representation of both controllers will be presented and in the last paragraph a first comparison between the two concepts is made.

§ 2.1 The controller of R.Kelly

A diagram of the control strategy of R.Kelly is shown in the figure below:

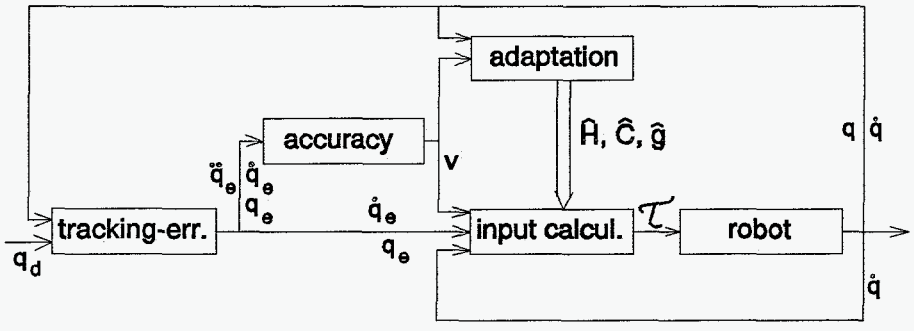

Figure 2.1: 'diagram of controller of R.Kelly'

The assumption is made that the robot can be described as:

$$H(q)\ddot{q} + C(q,\dot{q})\dot{q} + g(q) = \tau \qquad (2.1)$$

with:

q	: the n-dimensional column of joint displacements
τ	: the n-dimensional column of applied torques
$H(q)$	: the n×n symmetric positive definite manipulator inertia matrix
$C(q,\dot{q})\dot{q}$	: the n-dimensional column of centripetal and Coriolis forces
$g(q)$	: the n-dimensional column of gravitational forces

The input for the robot is calculated in the ***input***-block with:

$$\tau = \hat{H}(q,\hat{\theta})\{\ddot{q}_d + K_v\dot{q}_e + K_p q_e\} + \hat{C}(q,\dot{q},\hat{\theta})\dot{q} + \hat{g}(q,\hat{\theta}) - \hat{C}(q,\dot{q},\hat{\theta})v \qquad (2.2)$$

with:

q_d	: desired trajectory
q_e	: tracking error $q_e = q_d - q$
v	: measure of tracking accuracy
$\hat{\theta}$	: the m-dimensional column of the parameter estimates
$\hat{H}$, $\hat{C}$, $\hat{g}$	: estimates of H, C and g
K_v,K_p	: symmetric, positive definite matrices

In the ***accuracy***-part a measure v for the tracking accuracy is calculated with the following differential equation:

$$\dot{v} + \lambda v = -(\ddot{q}_e + K_v \dot{q}_e + K_p q_e) \tag{2.3}$$

If the input can be discribed by the linearity relation:

$$\tau = \Phi(q, \dot{q}, \ddot{q}_d + K_v \dot{q}_e + K_p q_e, v)\,\hat{\theta} \tag{2.4}$$

then these parameters can be computed in the ***adaptation***-block with:

$$\frac{\partial \hat{\theta}}{\partial t} = -\Gamma^{-1} \Phi^T v \tag{2.5}$$

where Γ is the adaptation gain matrix.

In equation 2.2 we saw four terms. The second and third term are to compensate the coriolis, centripetal and gravitational forces. If the parameters are equal to the actual values, then these forces will be compensated completely.
The first term will decrease the error to zero, if the parameters are correct. Because of parameter and model errors the fourth term has to be added, to guarantee stability.

To obtain an adaptation law, the assumption was made that the input could be written linear in the estimated parameters. Of course this isn't always the case. For those systems where it is not possible to write the input linear in the estimated parameters, it should be noticed that this adaptation law could cause instability.

§ 2.2 The controller of Slotine-Li

The controller of Slotine-Li looks much like the controller of R.Kelly. The adaptation parts are almost equal. The difference between them, however, is in the controller parts.
In figure 2.2 a diagram of the controller is given.

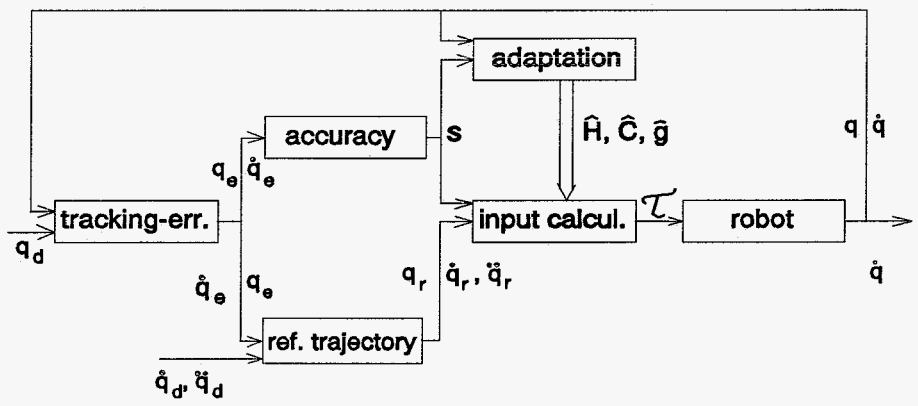

Figure 2.2: 'diagram of controller of Slotine-Li'

According to J.J.E. Slotine and W. Li [2], the following input can be used, if the robot matches description 2.1:

$$\tau = \hat{H}(q,\theta)\ddot{q}_r + \hat{C}(q,\dot{q},\theta)\dot{q}_r + \hat{g}(q,\theta) - K_d s \tag{2.6}$$

with:

$$\dot{q}_r = \dot{q}_d + \Lambda q_e$$

and:

$$q_e = q_d - q$$
$$s = \dot{q} - \dot{q}_r = -\dot{q}_e - \Lambda q_e$$

It is assumed that in this case the feedforward part of the input can be described by the linearity relation:

$$\hat{H}(q,\theta)\ddot{q}_r + \hat{C}(q,\dot{q},\theta)\dot{q}_r + \hat{g}(q,\theta) = Y(q,\dot{q},\dot{q}_r,\ddot{q}_r)\hat{\theta} \tag{2.7}$$

The adaptation law can now be written as:

$$\frac{\partial \hat{\theta}}{\partial t} = -\Gamma^{-1} Y^T(q,\dot{q},\dot{q}_r,\ddot{q}_r)\, s \tag{2.8}$$

Equation 2.7 exists of four terms. The first three terms are used for the feedforward compensation of the end-effector forces, while the term $K_d s$ regulates the tracking error and guarantees its convergence.
The restrictions mentioned in § 2.1, concerning the linearity of the input, apply here as well. So not all systems can be controlled with the use of this adaptation law.

§ 2.3 A comparison between the controllers

According to R.Kelly [1] the difference between the two controllers is found in the fact that his controller has a computed torque part with a feedback while the controller of Slotine-Li is a feedforward controller with a feedback.

The main difference is situated in the order of the controllers. The order of the controller of R.Kelly is one higher than the controller of Slotine-Li. This difference can be found in the use of a measure of tracking accuracy. Where R.Kelly uses a first order filtered measure , Slotine and Li use a linear algebraic relation. This results in an extra control parameter in case of R.Kelly. When comparing these controllers this extra parameter will be varied to find the optimal controller.

Chapter 3:

Simulations with the RT-manipulator

In this chapter the controller of R.Kelly and the controller of Slotine-Li will be applied to a R(otation) T(ranslation)-manipulator. First a model of the RT-robot will be derived. Then a trajectory will be chosen, followed by the estimation of the control parameters in paragraph 3.3. In paragraph 3.4 the simulation results are shown in case of various situations.

§ 3.1 Model of the RT-manipulator

To make a comparison between the control concept of Slotine-Li and the control concept of R.Kelly, both controllers are used in a simulation of a RT-manipulator, as proposed in E.Freund [3]. A simple drawing of the RT-manipulator is given below.

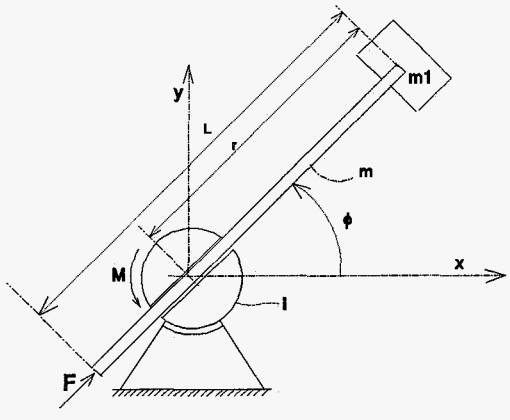

Figure 3.1: RT-robot

The RT-robot consists of a disk with moment inertia I and a rigid bar with lenght ℓ and homogeneously distributed mass m. If there is no friction, the bar can be pushed up and down inside the disk by force F(t) without resistance. The load at the end of the bar is a concentrated mass m_1. The disk can be rotated by torque M(t). The system has with two degrees of freedom, a rotation $\varphi(t)$ and a translation r(t).

The manipulator can be described with the following equations:

$$\theta_1 \ddot{r} - (\theta_1 r - \theta_2)\dot{\varphi}^2 = F \qquad (3.1)$$

$$(\theta_3 - 2\theta_2 r + \theta_1 r^2)\ddot{\varphi} + 2(\theta_1 r - \theta_2)\dot{r}\dot{\varphi} = M \qquad (3.2)$$

with:

$\theta_1 = m + m_1 = 15$ [kg]

$\theta_2 = \frac{1}{2} m \ell = 5$ [kg m]

$\theta_3 = I + \frac{1}{3} m \ell^2 = 8\frac{1}{3}$ [kg m^2]

§ 3.2 Desired trajectory of the RT-manipulator

The trajectory, which has to be followed by the manipulator, has to be a smooth function. A representative trajectory for a pick and place robot is a sine, with a straight line added to it. In the simulations the next trajectory is used:

- If $0 \le t \le 1.0$ [s]:

$$r_d = \frac{3}{4}t - \frac{3}{8\pi}\sin(2\pi t) + \frac{1}{4} \quad [m]$$

$$\varphi_d = \frac{\pi}{2}t - \frac{1}{4}\sin(2\pi t) \quad [rad]$$

- If $1.0 \le t \le 2.0$ [s]:

$$r_d = -\frac{3}{4}(t-2) + \frac{3}{8\pi}\sin(2\pi t) + \frac{1}{4} \quad [m]$$

$$\varphi_d = \frac{\pi}{2}t - \frac{1}{4}\sin(2\pi t) \quad [rad]$$

- If $2.0 \le t \le 3.0$ [s]:

$$r_d = \frac{3}{4}(t-2) - \frac{3}{8\pi}\sin(2\pi t) + \frac{1}{4} \quad [m]$$

$$\varphi_d = \frac{\pi}{2}t - \frac{1}{4}\sin(2\pi t) \quad [rad]$$

At first the trajectory was chosen, as above from 0 to 1 seconds, continued with $r_d = 1$ and $\varphi_d = \frac{1}{2}\pi$ from 1 tot 1.4 seconds (see L.J.W. v. Gerwen [4]). Because the parameters didn't converge at this time interval, the desired trajectory was enlarged with two seconds, as shown above.
This resulted in the following plots for r_d-t, φ_d-t en x-y :

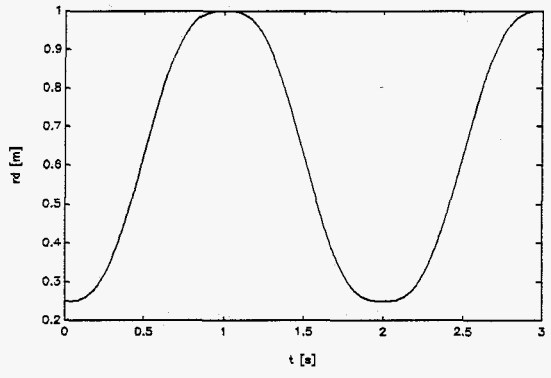

Figure 3.2: 'Desired radius'

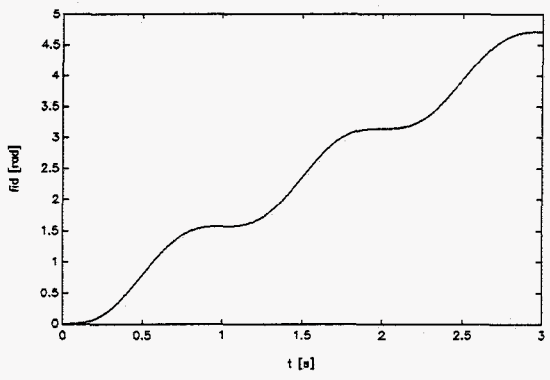

Figure 3.3: 'Desired angle'

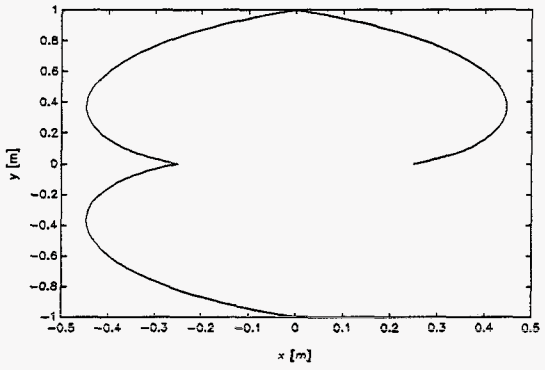

Figure 3.4: 'Desired x- and y-coördinates'

§ 3.3 Estimation of control parameters

Both controllers have to be tuned in such a manner, that they can be compared. To avoid a lot of experiments (to find the optimal parameters), I chose to tune them both in an equivalent way. To make the same choise for the PD-feedback of both controllers an equivalent tuning is obtained. Both controllers can be described as a Computed-torque part and a PD-feedback part, as illustrated in figure 3.5 .

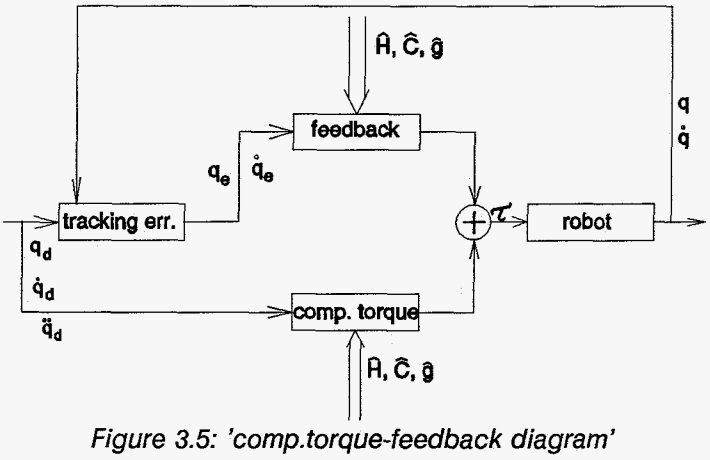

Figure 3.5: 'comp.torque-feedback diagram'

The assumption is made that the following relation is a solution of equation 2.3:

$$v = -(\dot{q}_e + A q_e) \qquad (3.3)$$

with:

$$A = \frac{K_P}{\lambda}$$

From equation 2.2 and 3.3 it can be derived in case of the controller of R. Kelly:

$$\tau = \hat{H}(q,\hat{\theta})\,\ddot{q}_d + \hat{C}(q,\dot{q},\hat{\theta})\,\dot{q}_d + \hat{g}(q,\hat{\theta}) + \hat{H}(q,\hat{\theta})\,K_v\,\dot{q}_e + [\hat{H}(q,\hat{\theta}) + \frac{1}{\lambda}\hat{C}(q,\dot{q},\hat{\theta})]\,K_p\,q_e \tag{3.4}$$

and in case of the controller of Slotine-Li equation 2.6 yields:

$$\tau = \hat{H}(q,\hat{\theta})\,\ddot{q}_d + \hat{C}(q,\dot{q},\hat{\theta})\,\dot{q}_d + \hat{g}(q,\hat{\theta}) + [\hat{H}(q,\hat{\theta})\Lambda + K_d]\,\dot{q}_e + \Lambda[\hat{C}(q,\dot{q},\hat{\theta}) + K_d]\,q_e \tag{3.5}$$

The following linearized equations in a stationary working point (r_0 ,φ_0) can be derived:

$$\theta_1 \ddot{r} = F \tag{3.6}$$

$$I_1 \ddot{\varphi} = M \tag{3.7}$$

with:

$$I_1 = \theta_3 - 2\theta_2 r_0 + \theta_1 r_0^2$$

If a PD-controller is designed, and the inputs are:

$$F = -\Delta_{d1}(\dot{r} - \dot{r}_d) - \Delta_{p1}(r - r_d) \tag{3.8}$$

$$M = -\Delta_{d2}(\dot{\varphi} - \dot{\varphi}_d) - \Delta_{p2}(\varphi - \varphi_d) \tag{3.9}$$

then the total system can be described (for both degrees of freedom) as:

$$\theta_1 \ddot{r} + \Delta_{d_1}\dot{r} + \Delta_{p_1} = \Delta_{d_1}\dot{r}_d + \Delta_{p_1} r_d \tag{3.10}$$

$$\theta_2 \ddot{\varphi} + \Delta_{d_2}\dot{\varphi} + \Delta_{p_2} = \Delta_{d_2}\dot{\varphi}_d + \Delta_{p_2}\varphi_d \tag{3.11}$$

This can be written as:

$$\ddot{q} + 2\beta\omega_0\dot{q} + \omega_0^2 q = 2\beta\omega_0\dot{q}_d + \omega_0^2 q_d \tag{3.12}$$

This yields:

$$\Delta_p = \begin{bmatrix} \Delta_{p1} & 0 \\ 0 & \Delta_{p2} \end{bmatrix} = \begin{bmatrix} \omega_0^2\theta_1 & 0 \\ 0 & \omega_0^2 I_1 \end{bmatrix} = \omega_0^2 H(q_0)$$

$$\Delta_d = \begin{bmatrix} \Delta_{d1} & 0 \\ 0 & \Delta_{d2} \end{bmatrix} = \begin{bmatrix} 2\beta\omega_0\theta_1 & 0 \\ 0 & 2\beta\omega_0 I_1 \end{bmatrix} = 2\beta\omega_0 H(q_0)$$

These two matrices are used in the controllers of R.Kelly and Slotine-Li as PD-feedback.

To find the control matrices (K_v ,K_p ,K_d and Λ), it is assumed that the estimated parameters are equal to the actual values.
Because we linearized in a stationary workpoint, all non linear terms in $\hat{C}$ are zero. Ergo $\hat{C}$ is zero (see appendix A).
Therefore:

- $\hat{H} = H(q_o)$
- $\hat{C} = 0\ I$

The control matrices K_v and K_p of R. Kelly are described by:

$$\hat{H}(q_0,\hat{\theta})K_v = \Delta_d = 2\beta\omega_0 H(q_0) \quad \Rightarrow \quad K_v = 2\beta\omega_0 I \tag{3.13}$$

$$\hat{H}(q_0,\hat{\theta})K_p = \Delta_p = \omega_0^2 H(q_0) \quad \Rightarrow \quad K_p = \omega_0^2 I \tag{3.14}$$

From equation 3.5 we obtain in case of Slotine-Li:

$$\hat{H}(q_0,\hat{\theta})\Lambda + K_d = \Delta_d = 2\beta\omega_0 H(q_0) \tag{3.15}$$

$$\Lambda K_d = \Delta_p = \omega_0^2 H(q_0) \tag{3.16}$$

If the two adaptive controllers are designed as PD-controllers, we find that if r_0 varies the control matrices of R. Kelly remain constant (since $\hat{C} = 0$ en $\hat{H} = H$), and the controller parameters of Slotine-Li change.
The most unfavourable working point is, where the gain matrices are the smallest. Then I_1, which only depends on r_0, is the smallest. This point, which is the centre of the bar with load, because in that point a torque causes the largest acceleration, is:

$$r_0 = \tfrac{1}{3}\ [m]$$

If the following choises are made of the eigenfrequency and dampingfactor:

$$\omega_0 = 10 \quad [rad/s]$$
$$\beta = 1 \quad [-]$$

, then the controller matrices of R. Kelly are given by:

$$K_v = \begin{bmatrix} 20 & 0 \\ 0 & 20 \end{bmatrix}$$

$$K_p = \begin{bmatrix} 100 & 0 \\ 0 & 100 \end{bmatrix}$$

and in case of the controller of Slotine-Li the matrices K_d and Λ are:

$$K_d = \begin{bmatrix} 150 & 0 \\ 0 & \frac{200}{3} \end{bmatrix}$$

$$\Lambda = \begin{bmatrix} 10 & 0 \\ 0 & 10 \end{bmatrix}$$

The adaptation gain matrices in both cases can be taken to be the same:

$$\Gamma^{-1} = \begin{bmatrix} 100 & 0 & 0 \\ 0 & 100 & 0 \\ 0 & 0 & 100 \end{bmatrix}$$

§ 3.4 Results of simulations with the RT-manipulator

In this paragraph we look at the simulation results. The simulations are devided in the following categories:

- Equivalent models: the model of the controller and the model of the proces are of the same order.
- Unmodelled dynamics: dynamics are present in the proces, but are not accounted for in the controller.
- Unmodelled dynamics + Friction: in the proces friction is present, whose parameters will be estimated during the adaptation.

In all the following simulations K_v ,K_p ,K_d and Λ have the same values as found in paragraph 3.3 .

3.4.1 Equivalent models

In this paragraph the simulations are executed without unmodelled dynamics and without friction. At this moment there is only one control parameter yet to be determined, i.e. λ. If we vary λ, we could determine the 'optimal' value of λ. Then the two controllers can be compared.
In appendix B simulations are shown with several values of λ. The optimal value was found to be:

$$\lambda = 25$$

In the same appendix the influence of the initial parameter estimates and the adaptation gain matrix are shown. If we draw both controllers in one figure, figures 3.6 and 3.7 can be obtained. The adaptation gain matrix was chosen to be:

$$\Gamma^{-1} = \begin{bmatrix} 100 & 0 & 0 \\ 0 & 100 & 0 \\ 0 & 0 & 100 \end{bmatrix}$$

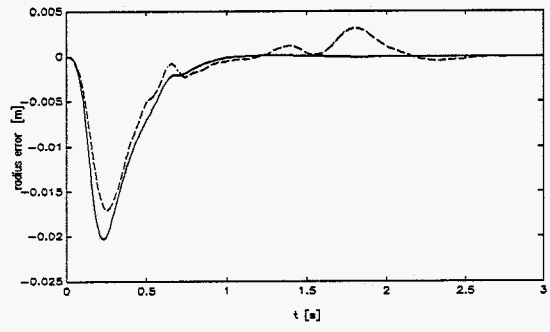

Figure 3.6: 'Radius error of both controllers'
——— : R.Kelly --- : Slotine-Li

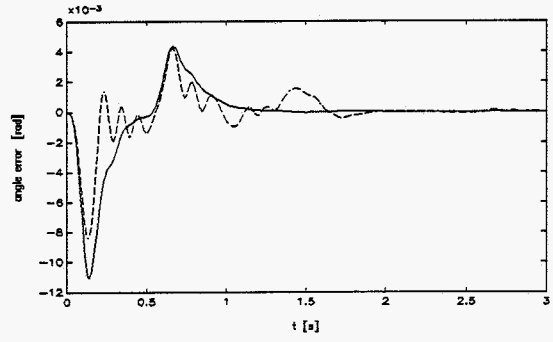

Figure 3.7: 'Angle error of both controllers'
——— : R.Kelly --- : Slotine-Li

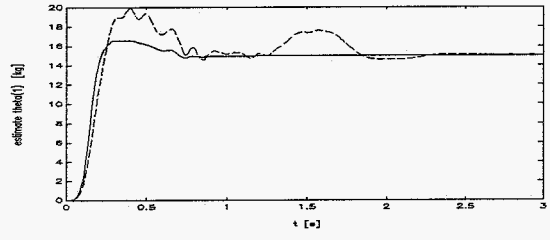

Figure 3.8: 'Estimate θ_1'
——— : R.Kelly --- : Slotine-Li

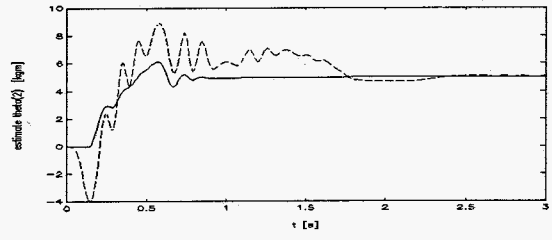

Figure 3.9: 'Estimate θ_2'
——— : R.Kelly --- : Slotine-Li

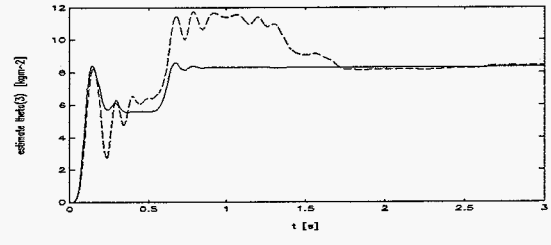

Figure 3.10: 'Estimate θ_3'
——— : R.Kelly --- Slotine-Li

From these figures we can conclude that both controllers in this situation almost have the same performance. The controller of R.Kelly, however, has a greater radius- and angle error in the beginning of the trajectory. The controller of R.Kelly makes greater angle errors between 0 sec. and 0.5 sec. After 0.5 second the errors, made by R.Kelly, are smaller than the errors of Slotine-Li.

3.4.2 Unmodelled dynamics

To compare the robustness of both controllers simulations are done with additional dynamics in the proces, which are not accounted for in the controller.
Up till now simulations were done with a motor producing a torque, which was computed by the controller. The motor however has got its own dynamics, which results in a torque different from what was calculated.

These dynamics can be described with the following differential equation:

$$\dot{T}_e = -\frac{r_a}{l_a}T_e - \frac{k_e k_t}{l_a}\omega + \frac{k_t}{l_a}u_r \qquad (3.15)$$

with:

T_e	=	motor torque
u_r	=	input voltage
ω	=	motor frequency
r_a	=	electrical resistance
l_a	=	self induction
k_e,k_t	=	motor constants

When the motor constants (r_a, l_a,k_e and k_t) were chosen realistic, AT-Matlab would make the time-integration step very small. Using an agreeable calculation accuracy, AT-matlab used a very long time to compute simulations with unmodelled dynamics. Because of these limitations, fictive values were used instead of realistic values. The values of the parameters are chosen so that the bandwidth of the motor is greater then the bandwidth of the controller, avoiding the chance of turning th system in an unstable proces. If we assume that ω and u_r are the inputs of the system and $l_a = 1$, then r_a represents the bandwidth. So r_a must be larger than 10. The chosen parameters are:

- $r_a = 25$
- $l_a = k_e = k_t = 1$

In appendix B simulations are shown with several values of λ. The optimal value was found to be:

$\lambda = 10$

Now both controllers will be compared. In these simulations the initial estimates are equal to the real values. The errors of radius and angle are shown in figure 3.11 and 3.12 .

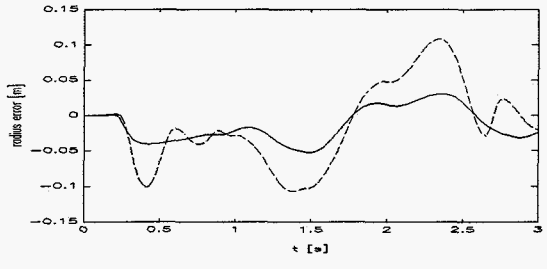

Figure 3.11: 'Radius error of both controllers'
—— : R.Kelly --- : Slotine-Li

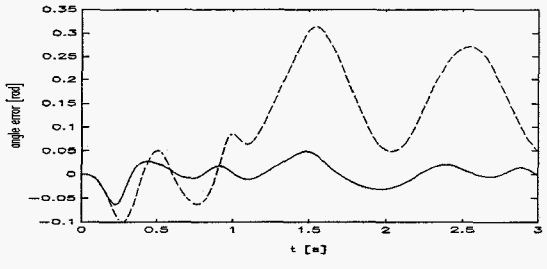

Figure 3.12: 'Angle error of both controllers'
—— : R.Kelly --- : Slotine-Li

Parameter estimates are shown in the figures below.

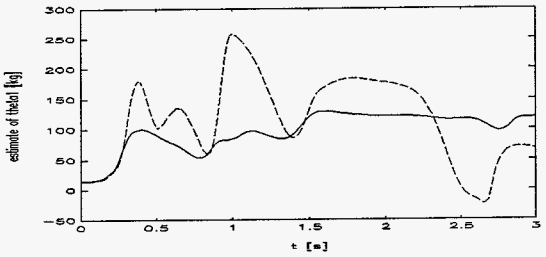

Figure 3.13: 'estim. θ_1'
——: R.Kelly --- : Slotine-Li

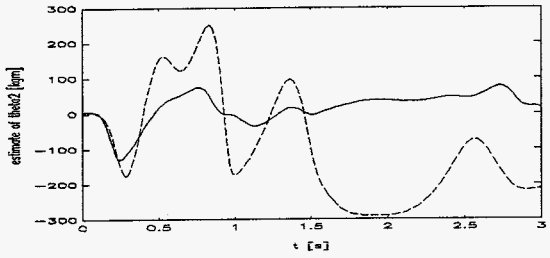

Figure 3.14: 'estim. θ_2'
——: R.Kelly --- : Slotine-Li

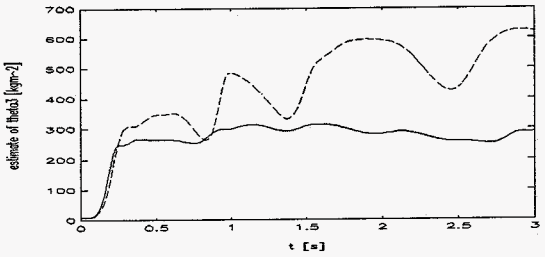

Figure 3.15: 'estim. θ_3'
——: R.Kelly --- : Slotine-Li

From these figures it can be concluded that the controller of R.Kelly has smaller errors than the controller of Slotine-Li. Also the parameter estimates are more stable in case of the controller of R.Kelly. If we compare these results with the figures shown in appendix B.2, we see that there is no significant difference between simulations with 0% or 100% of the initial estimates.
The system is a non-linear third order system, which is modelled in the controller by a second order system. This results in much larger values of the parameter estimates. The non-linearity of the actual system causes remaining errors. This is why the estimates don't converge.

3.4.3 Friction

In this subparagraph simulations are shown where unmodelled dynamics as well as friction are used.
Up till now the bar with load could be pushed up and down by force F(t) without resistance. In the following simulations two friction components are introduced:

$$F_c = -\theta_4 \, \text{sign}(\dot{r}) \tag{3.16}$$

$$F_v = -\theta_5 \dot{r} \tag{3.17}$$

with:

- θ_4 = 10 [N] : parameter of coulomb friction.
- θ_5 = 5 [Ns/m] : parameter of viscous friction.

Equation 2.1 changes in:

$$H(q)\ddot{q} + C(q,\dot{q})\dot{q} + g(q) = \tau + f_w \qquad (3.18)$$

with:

$$f_w = \begin{bmatrix} F_c + F_v \\ 0 \end{bmatrix}$$

In this case the column with parameter estimates has to be expanded to five parameter estimates and the adaptation gain-matrix has to be expanded to a 5×5 matrix.
In appendix B.3 simulations are shown with 50% friction compensation. The figures below show us simulations with 0% begin estimates.

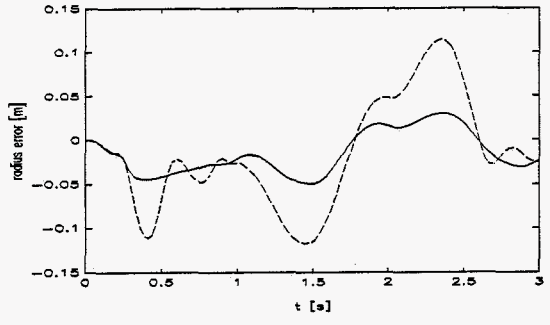

Figure 3.16: 'Radius error of both controllers'
—— : R.Kelly --- : Slotine-Li

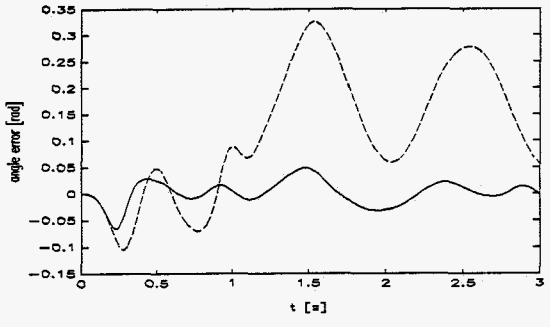

Figure 3.17: 'Angle error of both controllers'
—— : R.Kelly --- : Slotine-Li

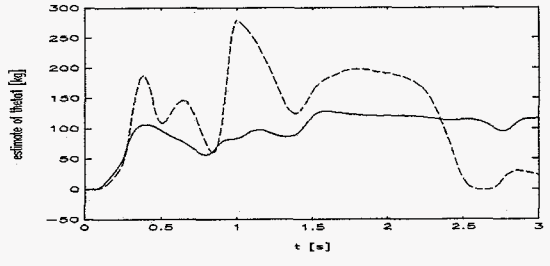

Figure 3.18: 'estimate θ_1'
—— : R.Kelly --- : Slotine-Li

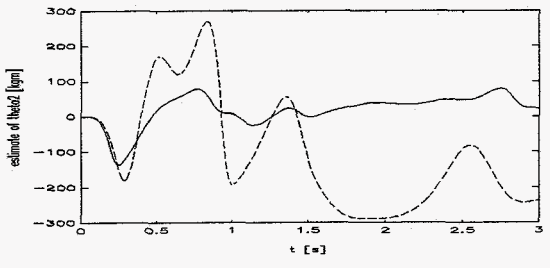

Figure 3.19: 'estimate θ_2'
—— : R.Kelly --- : Slotine-Li

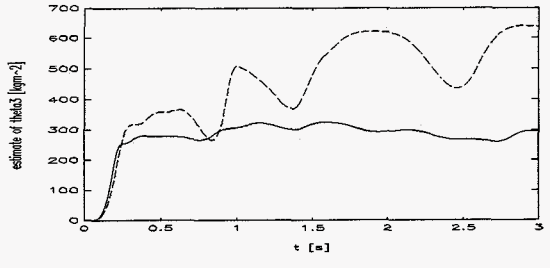

Figure 3.20: 'estimate θ_3'
—— : R.Kelly --- : Slotine-Li

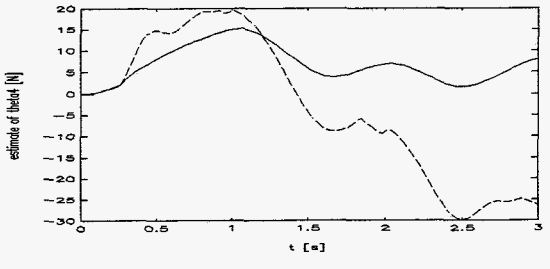

Figure 3.21: 'estimate θ_4'
—— : R.Kelly --- : Slotine-Li

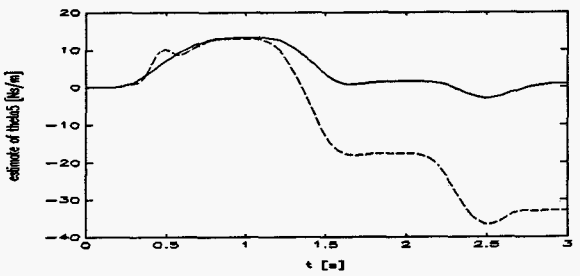

Figure 3.22: 'estimate θ_5'
——: R.Kelly --- : Slotine-Li

Simulations with unmodelled dynamics and friction are not very different from those with unmodelled dynamics alone. The reason for this is the fact that the influence of the friction on the tracking accuracy is small compared to the influence of the motor dynamics on the tracking accuracy.

§ 3.5 Conclusion

In subparagraph 3.4.1 we saw that there was not a great difference between the performances of the two controllers. If we take a look at the situation where unmodelled dynamics is fitted in, we see that the controller of R.Kelly performes better than the controller of Slotine-Li. The reason for this can be found in the paragraph 3.4 where the controllers were split up in to a computed torque part and a feedback. Here we saw that the controller matrices of R.Kelly were independent of the stationary workpoint.
Another reason is the difference in definition of the measure of the tracking accuracy. In both cases they are used to update the parameters and they are used as a feedback to guarantee the stability of the controller. R.Kelly uses a filtered definition of the measure v of tracking accuracy, so this is a less fluctuating signal than the measure s of accuracy, defined by Slotine-Li. This results in a less fluctuating parameter estimate and a less fluctuating feedback.
Because L.J.W. van Gerwen already investigated the performances of the PD-controller, when unmodelled dynamics were used, the controller of R.Kelly was only compared with the controller of Slotine-Li.

Chapter 4:

Simulation of the XY-table

Before applying the controller of R.Kelly on the XY-table, simulations are done to compare the performances of the controller of R.Kelly and the controller of Slotine-Li. In paragraph 4.1 the equations of motion will be derived. In paragraph 4.2 the gain matrices will be determined by reducing the control parameters to two parameters, i.e. ω_0 (eigenfrequency) and β (dampingfactor). Finally the simulation results will be shown.

§ 4.1 Description of the XY-table

A schematic representation is shown in figure 4.1. In figure 4.2 the system, used for simulations, is shown. Notice the difference between these figures concerning the definition of the positive y-direction.

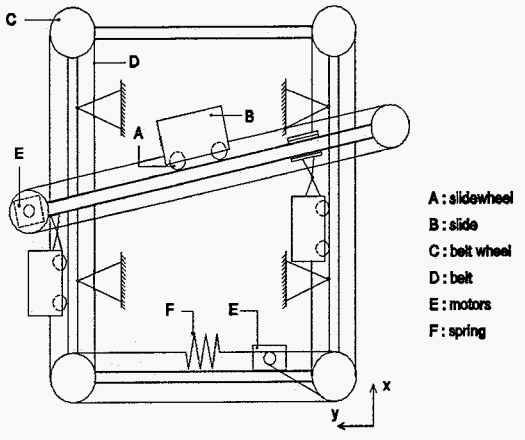

Figure 4.1: 'XY-table'

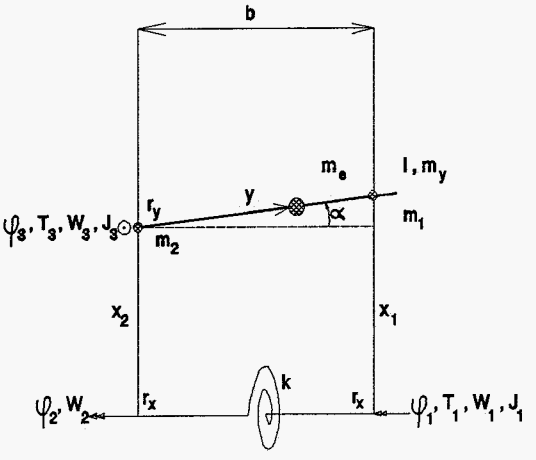

Figure 4.2: 'diagram of the XY-table'

The end-effector is a slide with mass m_e, which can move in the xy-plane by means of three slides. There are two slides in x-direction and one slide in y-direction. The belt wheels of the slideways in x-direction are connected with a torsion spring with stiffness k. This spring can be made rigid by turning on some screws.
There are three degrees of freedom, the rotations $\varphi_1(t)$, $\varphi_2(t)$ and $\varphi_3(t)$. If the torsion spring is active the rotations φ_1 and φ_2 will differ. The belt wheels of slideway one and three are both driven by a servomotor, with couples T_1 and T_3. Coulomb friction is modelled for movements along the slideways with torques W_1, W_2 and W_3. The equations of motion, which are used to simulate the real system, are given in appendix C. For both controllers a more simple model of the XY-table is used.

In this model there are only two degrees of freedom, because rotations φ_1 and φ_2 are assumed to be equal. This results in:

$$\theta_1 \ddot{\varphi}_1 = T_1 - \theta_3 \text{sign}(\dot{\varphi}_1) \tag{4.1}$$

$$\theta_2 \ddot{\varphi}_3 = T_3 - \theta_4 \text{sign}(\dot{\varphi}_3) \tag{4.2}$$

with:

θ_1	=	$2.34\ 10^{-3}$	[kgm^2]
θ_2	=	$2.80\ 10^{-4}$	[kgm^2]
θ_3	=	0.40	[Nm]
θ_4	=	0.02	[Nm]

These values were chosen the same as in L.J.W. van Gerwen [4], to compare the results of his study and the results in this report.

§ 4.2 Estimation of control parameters

To determine the control matrices K_v and K_p of the controller of R.Kelly and the control matrices K_d and Λ of the controller of Slotine-Li, a reduced model was used. As a reduced model equations 4.1 and 4.2 without the friction terms were used.

$$\theta_1 \ddot{\varphi}_1 = T_1 \tag{4.3}$$

$$\theta_2 \ddot{\varphi}_3 = T_3 \tag{4.4}$$

The controller of R.Kelly has the following form:

$$\tau = \hat{H}(q,\hat{\theta})\ddot{q}_d + \hat{H}(q,\hat{\theta})K_v\dot{q}_e + \hat{H}(q,\hat{\theta})K_p q_e \tag{4.5}$$

The controller of Slotine-Li has the following form:

$$\tau = \hat{H}(q,\hat{\theta})\ddot{q}_d + [\hat{H}(q,\hat{\theta})\Lambda + K_d]\dot{q}_e + \Lambda K_d q_e \tag{4.6}$$

The system- and controller matrices are given in appendix D.

Now a PD-feedback was designed, similar as in chapter 3. These PD-feedback matrices were used in the adaptive controllers of R.Kelly and of Slotine-Li.

The PD-feedback of the motor rotations are:

$$T_1 = -\Delta_{d1}(\dot{\varphi}_1 - \dot{\varphi}_{1d}) - \Delta_{p1}(\varphi_1 - \varphi_{1d}) \tag{4.7}$$

$$T_3 = -\Delta_{d3}(\dot{\varphi}_3 - \dot{\varphi}_{3d}) - \Delta_{p3}(\varphi_3 - \varphi_{3d}) \tag{4.8}$$

If we substitute equations 4.7 in 4.3 and 4.8 in 4.4, then the following equations can be derived:

$$\ddot{\varphi}_1 + \frac{\Delta_{d1}}{\theta_1}\dot{\varphi}_1 + \frac{\Delta_{p1}}{\theta_1}\varphi_1 = \frac{\Delta_{d1}}{\theta_1}\dot{\varphi}_{1d} + \frac{\Delta_{p1}}{\theta_1}\varphi_{1d} \tag{4.9}$$

$$\ddot{\varphi}_3 + \frac{\Delta_{d3}}{\theta_2}\dot{\varphi}_3 + \frac{\Delta_{p3}}{\theta_2}\varphi_3 = \frac{\Delta_{d3}}{\theta_2}\dot{\varphi}_{3d} + \frac{\Delta_{p3}}{\theta_2}\varphi_{3d} \tag{4.10}$$

These equations can be written in the following equation:

$$\ddot{\varphi} + 2\beta\omega_0\dot{\varphi} + \omega_0^2\varphi = 2\beta\omega_0\dot{\varphi}_d + \omega_0^2\varphi_d \tag{4.11}$$

This results in:

$$\Delta_p = \begin{bmatrix} \omega_0^2\theta_1 & 0 \\ 0 & \omega_0^2\theta_2 \end{bmatrix}$$

$$\Delta_d = \begin{bmatrix} 2\beta\omega_0\theta_1 & 0 \\ 0 & 2\beta\omega_0\theta_2 \end{bmatrix}$$

The eigenfrequency ω_0 and the damping factor were chosen the same as in L.J.W. van Gerwen [4]:

$$\omega_0 = 10 \quad \left[\frac{\text{rad}}{\text{s}}\right]$$

$$\beta = 1 \quad [-]$$

As in L.J.W. van Gerwen this results, in case of the controller of Slotine-Li in:

$$K_d = \Delta_d = \begin{bmatrix} 23.4 & 0 \\ 0 & 2.80 \end{bmatrix} 10^{-2}$$

$$\Lambda = K_d^{-1}\Delta_p = \begin{bmatrix} 5 & 0 \\ 0 & 5 \end{bmatrix}$$

Similar to chapter 3 we choose $H = \hat{H}$ to determine the control matrices of the controller of R.Kelly:

$$\hat{H}(q_0,\hat{\theta})K_v = \Delta_d \quad \Rightarrow \quad K_v = \begin{bmatrix} 20 & 0 \\ 0 & 20 \end{bmatrix}$$

$$\hat{H}(q_0,\hat{\theta})K_p = \Delta_p \quad \Rightarrow \quad K_p = \begin{bmatrix} 100 & 0 \\ 0 & 100 \end{bmatrix}$$

§ 4.3 Results of simulations with the XY-table

In L.J.W. van Gerwen [4] is shown that, when using only end-effector feedback, instability could occur. Therefore the displacements of the end-effector and the motor rotations were used in the feedback with weighing factors. Also the angular speed of the motors and end-effector velocity were used in a weighing criterium. L.J.W. van Gerwen showed us that good results could be achieved when using:

$$W_m = 0.4$$
$$W_e = 0.6$$

The XY-table was simulated with the controller of R.Kelly and with the controller of Slotine-Li. The desired trajectory , that was used, was chosen to be a circle:

$$x_d = 0.5 - 0.25\cos(2\pi t) \quad [m]$$
$$y_d = 0.5 + 0.25\cos(2\pi t) \quad [m]$$

When making the choise of the adaptation gain matrix, it is important to realise that the adaptation process must be slower than the control process to avoid instabilities. The adaptation gain matrix Γ was chosen as in L.J.W. van Gerwen [4]:

$$\Gamma^{-1} = \begin{bmatrix} 2.5\cdot10^{-7} & 0 & 0 & 0 \\ 0 & 2.5\cdot10^{-8} & 0 & 0 \\ 0 & 0 & 1\cdot10^{-1} & 0 \\ 0 & 0 & 0 & 1\cdot10^{-2} \end{bmatrix}$$

In appendix E the errors and parameter estimates are shown of the controller of R.Kelly when using several values of λ. For the simulation of the XY-table $\lambda = 10$ was chosen. In the figures 4.3 to 4.7 the errors and parameter estimates are shown.

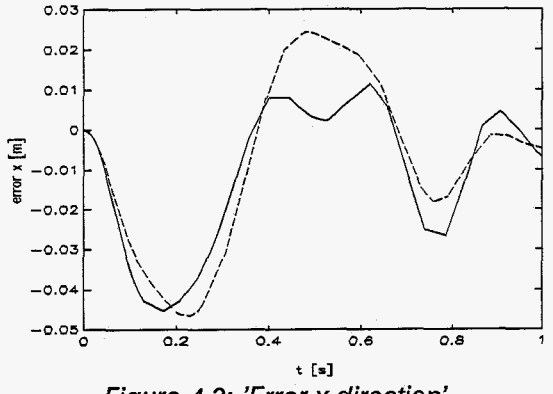

Figure 4.3: 'Error x-direction'
——: R.Kelly --- : Slotine-Li

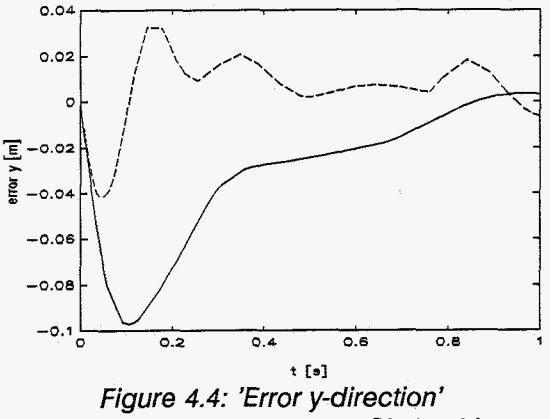

Figure 4.4: 'Error y-direction'
——: R.Kelly --- : Slotine-Li

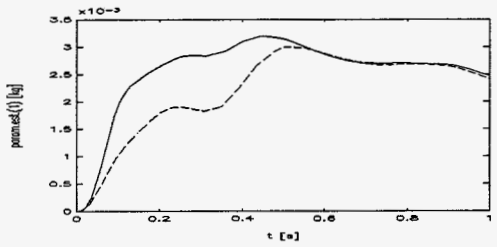

Figure 4.5: 'Estimate θ_1'
——— : R.Kelly --- : Slotine-Li

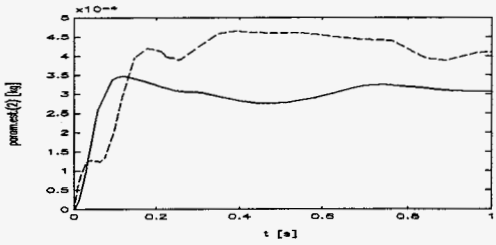

Figure 4.6: 'Estimate θ_2'
——— : R.Kelly --- : Slotine-Li

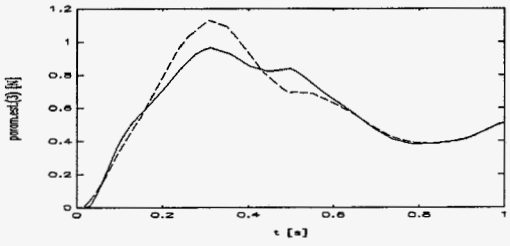

Figure 4.7: 'Estimate θ_3'
——— : R.Kelly --- : Slotine-Li

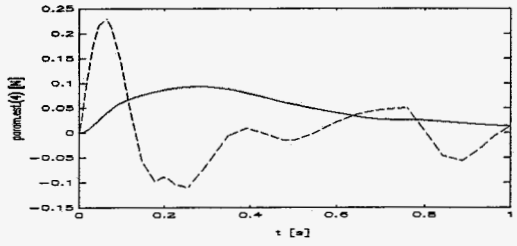

Figure 4.8: 'Estimate θ_4'
——— : R.Kelly --- : Slotine-Li

§ 4.4 Conclusions

Here we see a better performance of the controller of Slotine-Li in y-direction. Because the inputs of both controllers are similar, the reason must be found in the adaptation. While the other parameters converge to the same value, θ_2 and θ_4 are different in both cases. These two parameters determine the accuracy in y-direction.
These two parameters are biased, because of the torsion spring of the XY-table. This must also be the reason why the parameters do not converge. We have seen in chapter 3, that the used model in the controller is equal to the actual system, the parameters will converge to their actuel values. The torsion spring is the cause of the remainig errors, which in turn is the cause of the little fluctuations of the estimates.
Here too we can see that the estimations, in case of the controller of Slotine-Li, is more fluctuating.

Chapter 5:

Implementation on the XY-table

The results of chapter three and four show that the controller could be succesfully used to control the XY-table. In the following paragraph a description of the model is given, which was used for the controller. To compensate time delays and discretization effects a Kalman filter was used. The design of the Kalman filter will be discussed in paragraph 5.2. In 5.3 the tuning of the controllers will be shown and in 5.4 the results of some experiments will be given.

§ 5.1 Description of the XY-table

The implementation of the controller of R.Kelly was done on the same XY-table used by L.J.W. van Gerwen [4]. Because the optical measurement system, which measures the position of the end-effector, was broken, only the servomotor position could be used as feedback.

To design the two controllers a simple model of the XY-table was used:

$$\theta_1 \ddot{x} = F_1 - \theta_3 \operatorname{sign}(\dot{x}) \tag{5.1}$$

$$\theta_2 \ddot{y} = F_2 - \theta_4 \operatorname{sign}(\dot{y}) \tag{5.2}$$

with:

θ_1 = 46.5 [kg]
θ_2 = 4.3 [kg]
θ_3 = 50.0 [N]
θ_4 = 15.0 [N]

From the results we will see that these parameters do not correspond to the exact values.

§ 5.2 Kalman observer

During the control of the XY-table only servomotor rotations could be measured. To obtain the angular speed of the motor, there are two options. One is numerical differentiation of the rotations. This leads to two kinds of errors. First, measurement errors of the rotations cause errors at the size of the difference in rotation devided by the time interval. A larger time interval will produce smaller errors due to measuring errors. Secondly, differentiation gives an estimate of the angular speed at the point of time in the middle of the interval, not at the end of the interval. This causes a time delay in the estimated angular speed of half a time interval. A larger interval results in a larger time delay. From this we can conclude that there is an optimal time interval.

Because the motor rotations are measured and the angular speeds are determined by differentiation, the computer has to calculate the inputs to make the end-effector track the desired trajectory. This causes some time delay with respect to the inputs.

The above effects can be reduced by using a Kalman observer. The Kalman observer determines the speed not only with the measured rotations but also with the knowledge of the dynamics. It estimates the position and speed one sample ahead using the measurements, the last estimated position, the last estimated speed, the last inputs and the knowledge of the dynamics. The results are used to calculate the input, which are applied at the time on which the position and speed are predicted. During the experiments the same Kalman observer was used as designed by L.J.W. van Gerwen [4]. In appendix F the design of the Kalman observer is shown.

§ 5.3 Estimation of control parameters

Apart from the build-in possibility to use a rigid or a flexible bar, other unmodelled dynamics are present which can not be influenced. These are:

- Harmonic friction terms in X- and Y direction due to bad bearings.
- Backlash in one of the bearings in X direction.
- Extra flexibility caused by little springs used in the transmission.
- When the belts touch the sides of the belt wheels, the friction changes.
- Motors and amplifiers have their own dynamics, which are not modelled.
- The sampling frequentie influences the error made by the Kalman filter.

As mentioned in L.J.W. van Gerwen [4], unmodelled dynamics impose a limit on the gain matrices of the controllers. To find the optimal value for the control matrices a simplified model shall be used, with parameters ω_0 and β. The input can be written as a PD-feedback:

$$F_1 = -\Delta_{d1}(\dot{x} - \dot{x}_d) - \Delta_{p1}(x - x_d) \tag{5.3}$$

$$F_3 = -\Delta_{d1}(\dot{y} - \dot{y}_d) - \Delta_{p1}(y - y_d) \tag{5.4}$$

If we substitute 5.3 in 5.1 and 5.4 in 5.2, the following linearized equations can be obtained:

$$\ddot{x} + 2\beta_x\omega_{0x}\dot{x} + \omega_{0x}^2 x = 2\beta_x\omega_{0x}\dot{x}_d + \omega_{0x}^2 x_d \tag{5.5}$$

$$\ddot{y} + 2\beta_y\omega_{0y}\dot{y} + \omega_{0y}^2 y = 2\beta_y\omega_{0y}\dot{y}_d + \omega_{0y}^2 y_d \tag{5.6}$$

with:

- ω_{0x}, ω_{0y} : eigenfrequencies in x- and y-direction
- β_x, β_y : damping factors in x- and y-direction

As found in L.J.W. van Gerwen [4] the control matrices of Slotine are:

$$K_p = \begin{bmatrix} \omega_{0x}^2\theta_1 & 0 \\ 0 & \omega_{0y}^2\theta_2 \end{bmatrix}$$

$$K_d = \begin{bmatrix} 2\beta_x\omega_{0x}\theta_1 & 0 \\ 0 & 2\beta_y\omega_{0y}\theta_2 \end{bmatrix}$$

If we assume, as in chapter three and four, that $H=\hat{H}$, then the matrices in case of Kelly are:

$$\Delta_d = \begin{bmatrix} 2\beta_x\omega_{0x} & 0 \\ 0 & 2\beta_y\omega_{0y} \end{bmatrix} H(q_0) = \hat{H}(q_o,\hat{\theta})K_v \quad \Rightarrow \quad K_v = \begin{bmatrix} 2\beta_x\omega_{0x} & 0 \\ 0 & 2\beta_y\omega_{0y} \end{bmatrix}$$

$$\Delta_p = \begin{bmatrix} \omega_{0x}^2 & 0 \\ 0 & \omega_{0y}^2 \end{bmatrix} H(q_0) = \hat{H}(q_o,\hat{\theta})K_p \quad \Rightarrow \quad K_p = \begin{bmatrix} \omega_{0x}^2 & 0 \\ 0 & \omega_{0y}^2 \end{bmatrix}$$

§ 5.4 Results of experiments with the XY-table

Experiments with the controllers on the XY-table were done in two cases:

- Experiments with a rigid system, i.e. the torsion spring was *not* operational.
- Experiments with a flexible system, i.e. the torsion spring was operational.

In both cases two trajectories were used:

- a straight line : $x_d = y_d = M - R\cos(2\pi ft)$ (diagonal)
- a circle : $x_d = M - R\cos(2\pi ft)$

  $y_d = M - R\cos(2\pi ft + \frac{\pi}{2})$

  with: M=0.8 [m] ; R=0.15 [m] ; f=1 [Hz]

5.4.1 Experiments with the rigid system

When using a sampling time T_s of 8 ms chattering occured at ω_0= 5 Hz. Therefore experiments were done with controller settings based on:

$$\omega_{0x} = \omega_{0y} = 4\cdot 2\pi \ \frac{\text{rad}}{\text{s}}$$

$$\beta_x = \beta_y = 0.7 \ [-]$$

If we first look at experiments with the diagonal as trajectory, the figures 5.1 to 5.6 were obtained. In these figures λ was chosen twenty after minimization of a quadratic criterium (see appendix G). The begin estimates were chosen equal to the values given in paragraph 5.1.

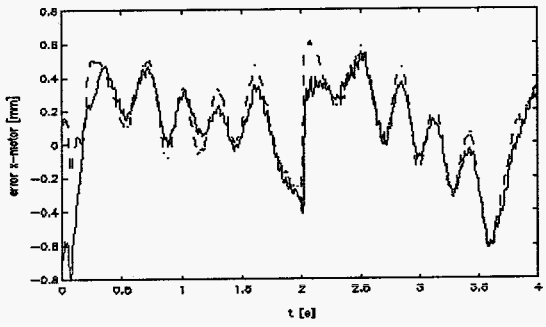

Figure 5.1: 'error of x-motor'
——— : Slotine-Li --- : R.Kelly

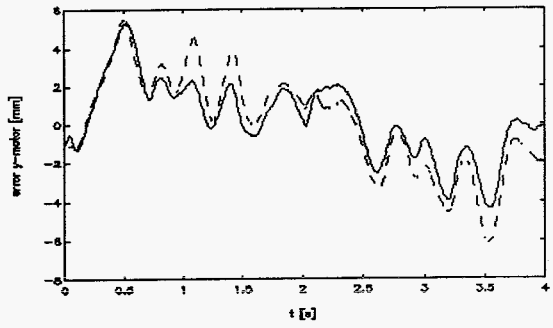

Figure 5.2: 'Error y-motor'
——— : Slotine-Li --- : R.Kelly

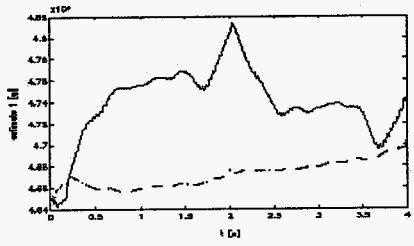

Figure 5.3: 'estimate θ_1'
——— : Slotine-Li --- : R.Kelly

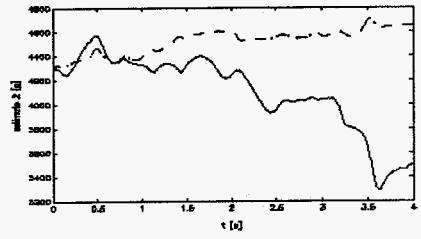

Figure 5.4: 'Estimate θ_2'
——— : Slotine-Li --- : R.Kelly

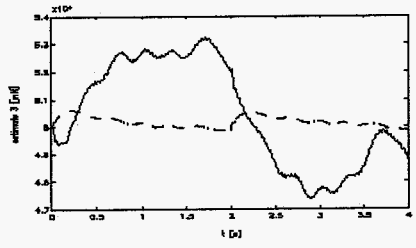

Figure 5.5: 'estimate θ_3'
——— : Slotine-Li --- : R.Kelly

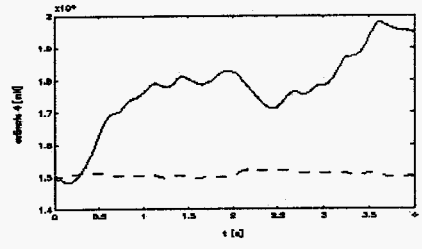

Figure 5.6: 'estimate θ_4'
——— : Slotine-Li --- : R.Kelly

From these figures we can conclude that the difference between the performances of the controllers is minimal. The controller of Slotine-Li has a slightly better performance, with respect to the error. The behaviour of the parameter estimation however is very different. The estimations in case of Slotine-Li are very fluctuating, while the estimations of R.Kelly are not.
Also in case of both controllers the estimations don't seem to converge to the same value. Because the inputs of the controller are very similar, the difference must be found in the difference between the used adaptation laws.

Experiments with the circle as desired trajectory result in figures 5.7 to 5.11. After some experiments with different values of λ, the controller of R.Kelly had the 'optimal' tuning with $\lambda=5$. It should be noticed that with another desired trajectory λ could be different, since λ was twenty in case of the diagonal.

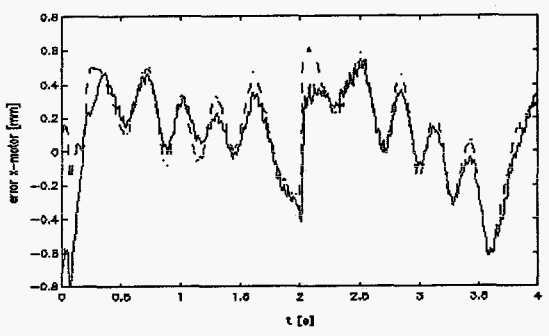

Figure 5.7: 'Error x-motor'
——: Slotine-Li --- : R.Kelly

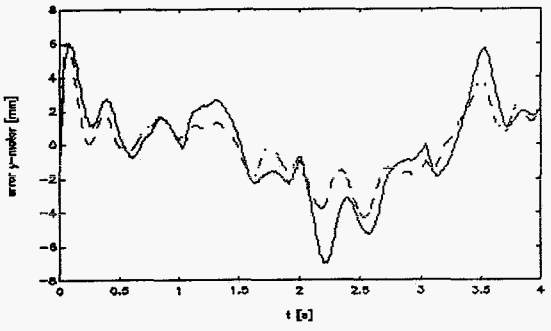

Figure 5.8: 'Error y-motor'
——: Slotine-Li --- : R.Kelly

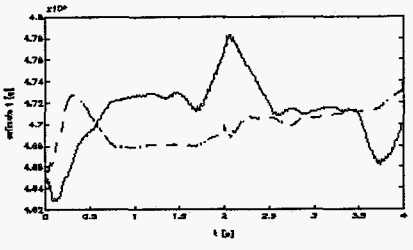

Figure 5.9: 'Estimate θ_1'
——: Slotine-Li --- : R.Kelly

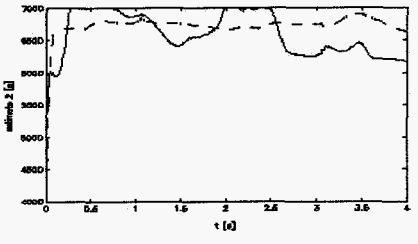

Figure 5.10: 'Estimate θ_2'
——: Slotine-Li --- : R.Kelly

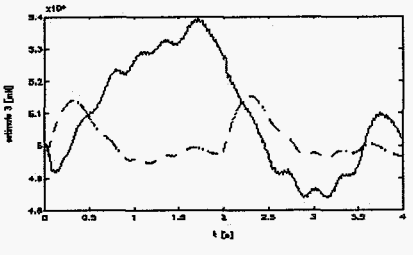

Figure 5.11: 'Estimate θ_3'
——: Slotine-Li --- : R.Kelly

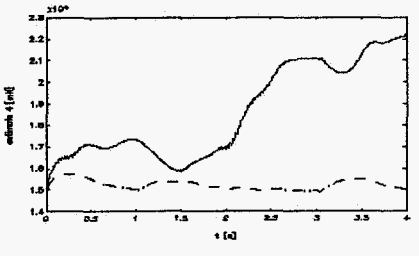

Figure 5.12: 'Estimate θ_4'
——: Slotine-Li --- : R.Kelly

Now we see that, especially in y-direction, the controller of R.Kelly has a better performance than the controller of Slotine-Li. The reason for this difference can be found in the estimations of the parameters. The only difference between the controllers is now the adaptation, while the control inputs are the same (a computed torque with a PD-feedback). We can see that the estimation of θ_1 and θ_2 differs from the estimation, when using a diagonal as a desired trajectory. Because the other parameters are estimated almost the same, when using different trajectories, this must be the reason why, in case of a circle as desired trajectory, the controller of R.Kelly is slightly better.
The estimation is trajectory dependent, because the trajectories are positioned differently in the XY-plane. These different positions result in different parameters of the friction.

The fluctuations of the parameter estimates, in case of the controller of R.Kelly, are smaller than those of the controller of Slotine-Li. The reason for this is found in the defenition of the measure of tracking accuracy. In case of the controller of R.Kelly this measure has a first order filtered definition.

This first order definition will result in a filtered measure with less high frequencies. This again results in estimates with less high frequencies.

5.4.2 Experiments with the flexible system

During these experiments only the rigid bar was replaced by the torsion spring. All the rest -like trajectories, kalman observer, model and sampling freqency- remained the same. As noticed in L.J.W. van Gerwen an eigenfrequency of 4 [Hz] will cause chattering, because in this case a torsion spring is used. Experiments showed that the following eigenfrequencies and damping factors in x-direction were the maximum values without causing any chattering:

Controller of R.Kelly:

$$\omega_{0x} = 3.5 \cdot 2\pi \quad \left[\frac{\text{rad}}{\text{s}}\right]$$
$$\beta_x = 0.7 \quad [-]$$

Controller of Slotine-Li:

$$\omega_{0y} = 2.5 \cdot 2\pi \quad \left[\frac{\text{rad}}{\text{s}}\right]$$
$$\beta_y = 0.7 \quad [-]$$

The choise of the adaptation gain matrix is not important as long as the adaptation process is slower then the control proces. In this situation the adaptation gain matrix was chosen the same as in 5.4.1.

In figure 5.13 to 5.17 the errors and parameter estimates are plotted,using the diagonal as desired trajectory.

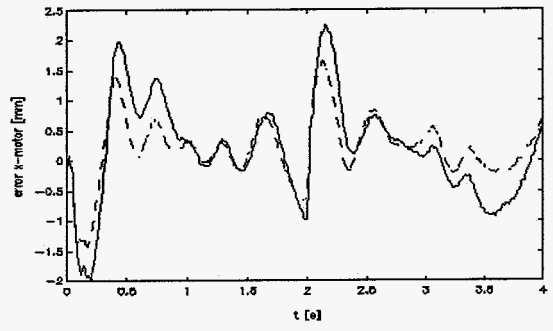

Figure 5.13: 'Error x-motor'
——: Slotine-Li --- : R.Kelly

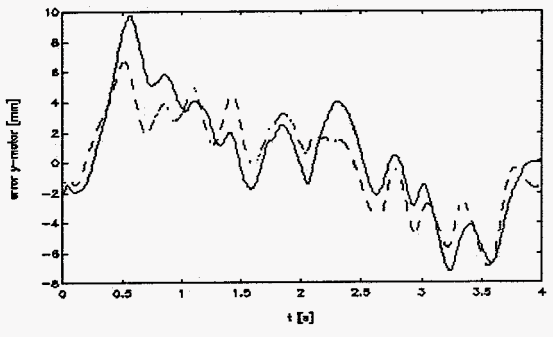

Figure 5.14: 'Error y-motor'
——: Slotine-Li --- : R.Kelly

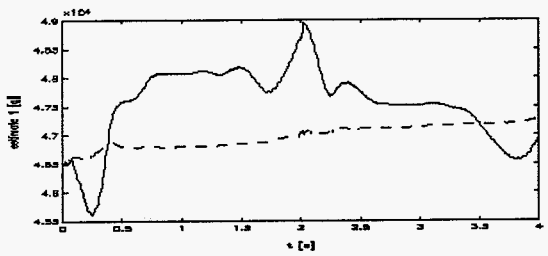

Figure 5.15: 'Estimate θ_1'
——— : Slotine-Li --- : R.Kelly

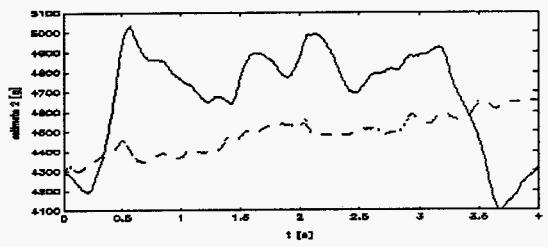

Figure 5.16: 'Estimate θ_2'
——— : Slotine-Li --- : R.Kelly

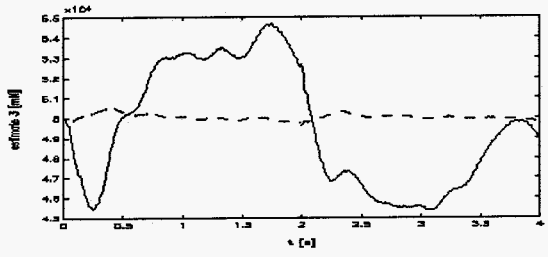

Figure 5.17: 'Estimate θ_3'
——— : Slotine-Li --- : R.Kelly

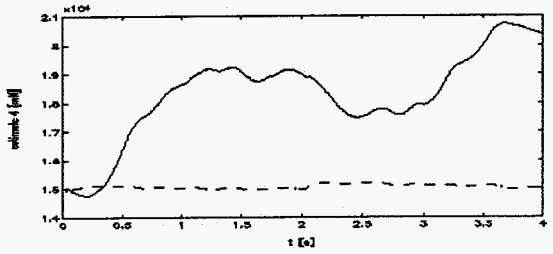

Figure 5.18: 'Estimate θ_4'
——— : Slotine-Li --- : R.Kelly

Figure 5.13 shows us that the error in x-direction, made by R.Kelly, is much smaller than the error made by the controller of Slotine-Li. This has to do with the fact that, because the chosen eigenfrequency of the controller of R.Kelly is larger, the P- and D-feedback matrices of R.Kelly are larger than the P- and D-feedback matrices of the controller of Slotine-Li. The performances in y-direction are almost the same. The errors, made by the controller of R.Kelly, are a bit smaller.
Figures 5.15 to 5.18 show us again that the estimates of the parameters are less fluctuating in case of the controller of R.Kelly, than in case of the controller of Slotine-Li.

In the figures 5.19 to 5.24 errors and parameter estimates are shown of experiments, when using the circle as desired trajectory.

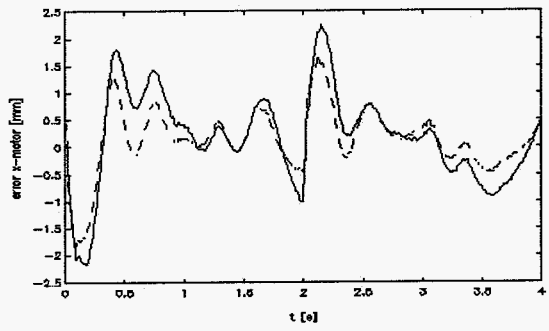

Figure 5.19: 'Error x-motor'
——— : Slotine-Li --- : R.Kelly

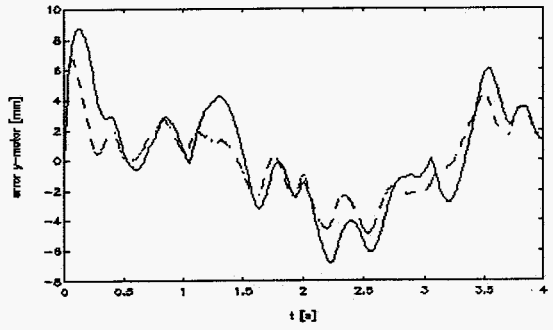

Figure 5.20: 'Error y-motor'
——— : Slotine-Li --- : R.Kelly

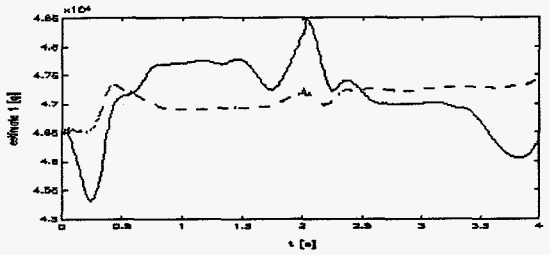

Figure 5.21: 'Estimate θ_1'
—— : Slotine-Li --- R.Kelly

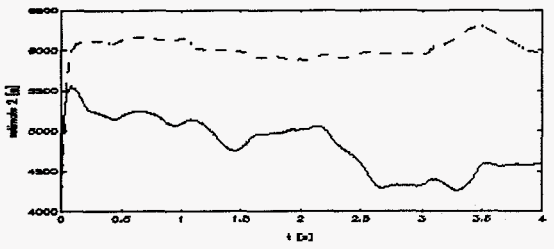

Figure 5.22: 'Estimate θ_2'
—— : Slotine-Li --- : R.Kelly

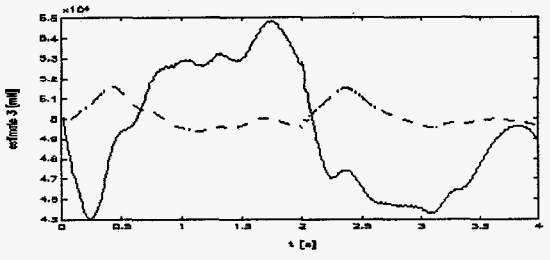

Figure 5.23: Estimate θ_3'
—— : Slotine-Li --- : R.Kelly

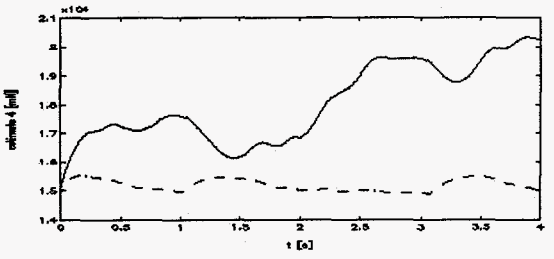

Figure 5.24: Estimate θ_4'
—— : Slotine-Li --- : R.Kelly

§ 5.5 Conclusions

Experiments with the rigid XY-table show that the performances of the controllers don't differ from each other. Experiments with the flexible XY-table show that the controller of R.Kelly is more robust than the controller of Slotine-Li. Also the tracking accuracy is slightly better in case of the controller of R.Kelly.

The parameter estimates in case of the controller of R.Kelly don't fluctuate as much as the estimates of the controller of Slotine-Li. As already explaned, this is caused by the first order filtered definition of the measure of tracking accuracy, in case of the controller of R.Kelly.

After convergence there still remain some fluctuations of the parameter estimates. This is caused by the unmodelled dynamics and the measurement noise. If a better model is used, a better tracking accuracy will be achieved. A higher sample frequency will also result in a better tracking accuracy, because it results in smaller speed estimation errors, made by the Kalman observer.

The chattering response of the XY-table is caused by the dynamics of the controlled XY-table, which consist of three parts. The first part is the XY-table itself. When using the flexible system, chattering will occur at smaller values of ω_0, than when using the rigid system. The second part is the controller. High gain matrices, i.e. large values of ω_0, result in a chattering respons. The third part is the Kalman observer. Chattering will occur, when using low sampling frequencies. These three parts are influenced by eachother. When the flexible system is used, the choice of the gain matrices has to be smaller. When higher sample frequencies are used, the gain matrices may chosen larger.

Chapter 6:

Conclusions and recommendations

In this chapter the most important conclusions are summarized and recommendations, for further experiments and research, are given.

- Simulations show, that the controller designed by R.Kelly can be succesfully implemented in flexible manipulators. There was, however, no big difference between the tracking accuracy, when the controllers were applied to the rigid system.
  The experiments showed, that compared to the controller of Slotine-Li, the controller of R.Kelly is more robust. Also the tracking accuracy was better in case of the controller of Kelly, when using the torsion spring.

- The behaviour of the parameter estimates was very different, when using the two controllers. The controller of Slotine-Li showed a very fluctuating estimate behaviour, while the controller of Kelly did not show such a fluctuating behaviour. The reason for this can be found in the definitions of measure of tracking accuracy, used by the controllers. The first order filtered definition of R.Kelly, results in estimates with less high frequencies.
  Increasing the adaptaion gain matrix resulted in a faster and more fluctuating behaviour of the estimation.

- The tracking accuracy of the controllers didn't differ much, when a rigid XY-table was used. The reason can be found in the fact, that the inputs the controllers were both computed torques with PD-feedback, when applying them to the XY-table. Other results may be obtained, when applying the controllers to systems,which do have centripetal- and Coriolis forces. In such a situation the full capacities of both controllers can be compared. The simulations of chapter three show, that the controller of R.Kelly looks very promising in that respect.

- When the gain matrices of the PD-feedback were chosen too large, a chattering response of the XY-table occured. As already explaned in chapter 5, this is caused by the errors of the speed estimation and unmodelled dynamics. A higher sampling frequency reduces the errors of the speed estimation. Improving the model, in the Kalman observer and the controller, results in a better speed estimation and less unmodelled dynamics.

- The optical measurement system, which measured the end-effector position, could not be used during this study. Therefore only the measurements of the motor positions were used. When the end-effector position measurements are available, it would be possible to compare the controllers again. To avoid instability a weighing methode could be used as proposed by L.J.W. van Gerwen.

- The unmodelled dynamics are the reason of remaining tracking errors and the remaining fluctuations of the parameter estimates after "convergence". Beside the torsion spring other unmodelled dynamics are present like backlash in one of the bearings, harmonic friction and dynamics of the motors and amplifier.

- In literature a lot of robust controllers are proposed. Further research should be done into their feasibility, their performance and their robustness. This can be done by implementing them in the XY-table and by comparing them with the controllers of Slotine-Li and R.Kelly.

Appendix A:

System and controller matrices for the RT-Robot

The matrices of equation 2.1 in case of the RT-manipulator are:

$$H = \begin{bmatrix} \theta_1 & 0 \\ 0 & \theta_3 + 2\theta_2 r + \theta_1 r^2 \end{bmatrix} \qquad C = \begin{bmatrix} 0 & -(\theta_1 r - \theta_2)\dot{\varphi} \\ (\theta_1 r - \theta_2)\dot{\varphi} & (\theta_1 r - \theta_2)\dot{r} \end{bmatrix}$$

$$g = \begin{bmatrix} 0 \\ 0 \end{bmatrix} \qquad q = \begin{bmatrix} r \\ \varphi \end{bmatrix} \qquad \tau = \begin{bmatrix} F \\ M \end{bmatrix}$$

In case of the controller of R.Kelly the input is given by equation 2.2. Each part can be written linear in the estimates:

$$\hat{H}(q,\hat{\theta})\,[\ddot{q}_d + K_v\dot{q}_e + K_p q_e] = \begin{bmatrix} \ddot{r}_d + K_{v_1}\dot{r}_e + K_{p_1} r_e & 0 & 0 \\ r^2\{\ddot{\varphi}_d + K_{v_2}\dot{\varphi}_e + K_{p_2}\varphi_e\} & -2r\{\ddot{\varphi}_d + K_{v_2}\dot{\varphi}_e + K_{p_2}\varphi_e\} & \ddot{\varphi}_d + K_{v_2}\dot{\varphi}_e + K_{p_2}\varphi_e \end{bmatrix}\hat{\theta}$$

$$\hat{C}(q,\dot{q},\hat{\theta})\,\dot{q} = \begin{bmatrix} -r\dot{\varphi}^2 & \dot{\varphi}^2 & 0 \\ 2r\dot{r}\dot{\varphi} & -2\dot{r}\dot{\varphi} & 0 \end{bmatrix}\hat{\theta}$$

$$-\hat{C}(q,\dot{q},\hat{\theta})\,v = \begin{bmatrix} r\dot{\varphi}v_2 & -\dot{\varphi}v_2 & 0 \\ -r\dot{\varphi}v_1 - r\dot{r}v_2 & \dot{\varphi}v_1 + \dot{r}v_2 & 0 \end{bmatrix}\hat{\theta}$$

with:

$$v = \begin{bmatrix} v_1 \\ v_2 \end{bmatrix} \quad ; \quad \hat{\theta} = \begin{bmatrix} \hat{\theta}_1 \\ \hat{\theta}_2 \\ \hat{\theta}_3 \end{bmatrix}$$

Together with equation 2.4, this yields:

$$\Phi = [\Phi_1 \;\; \Phi_2 \;\; \Phi_3] \qquad \textbf{(A.1)}$$

with:

$$\Phi_1 = \begin{bmatrix} 1 & 0 \\ 0 & r^2 \end{bmatrix}(\ddot{q}_d + K_v\dot{q}_e + K_p q_e) + \begin{bmatrix} -r\dot{\varphi}^2 + r\dot{\varphi}v_2 \\ 2r\dot{r}\dot{\varphi} - r\dot{\varphi}v_1 - r\dot{r}v_2 \end{bmatrix}$$

$$\Phi_2 = 2r\begin{bmatrix} 0 & 0 \\ 0 & -1 \end{bmatrix}(\ddot{q}_d + K_v\dot{q}_e + K_p q_e) + \begin{bmatrix} \dot{\varphi}^2 - \dot{\varphi}v_2 \\ -2\dot{r}\dot{\varphi} + \dot{\varphi}v_1 + \dot{r}v_2 \end{bmatrix}$$

$$\Phi_3 = \begin{bmatrix} 0 & 0 \\ 0 & 1 \end{bmatrix}(\ddot{q}_d + K_v\dot{q}_e + K_p q_e)$$

When friction is used in the simulations, the column with parameter estimates is expanded with two friction elements:

$$\hat{\theta} = \begin{bmatrix} \hat{\theta}_1 \\ \hat{\theta}_2 \\ \hat{\theta}_3 \\ \hat{\theta}_4 \\ \hat{\theta}_5 \end{bmatrix}$$

Φ is expanded in the following way:

$$\Phi = \begin{bmatrix} \Phi_1 & \Phi_2 & \Phi_3 & \Phi_4 \end{bmatrix} \qquad \textbf{(A.2)}$$

with:

$$\Phi_4 = \begin{bmatrix} -\text{sign}(\dot{r}) & -\dot{r} \\ 0 & 0 \end{bmatrix}$$

In case of Slotine-Li, Y is given by L.J.W. van Gerwen [4]:

$$Y = \begin{bmatrix} \ddot{r}_r - r\dot{\varphi}\dot{\varphi}_e & \dot{\varphi}\dot{\varphi}_r & 0 \\ r^2\ddot{\varphi}_r + r\dot{\varphi}\dot{r}_r & -2\ddot{\varphi}_r - \dot{r}\dot{\varphi}_r & \ddot{\varphi}_r \end{bmatrix}$$

with:

$$\begin{aligned} \dot{r}_r &= \dot{r}_d - \Lambda_{11} r_e \\ \dot{\varphi}_r &= \dot{\varphi}_d - \Lambda_{22} \varphi_e \end{aligned}$$

With friction Y is:

$$Y = \begin{bmatrix} \ddot{r}_r - r\dot{\varphi}\dot{\varphi}_e & \dot{\varphi}\dot{\varphi}_r & 0 & -\text{sign}(\dot{r}) & -\dot{r} \\ r^2\ddot{\varphi}_r + r\dot{\varphi}\dot{r}_r & -2\ddot{\varphi}_r - \dot{r}\dot{\varphi}_r & \ddot{\varphi}_r & 0 & 0 \end{bmatrix}$$

Appendix B:

Simulations with the RT-manipulator

In this appendix some additional results are shown, which are not essential to the explanation of the investigation. They only to a better insight in the behaviour of the controller.

§ B.1 Equivalent models

To determine the optimal value of λ, simulations are done with varying λ.
In table 3.1 on the next page the values of the control parameters are given and in figures 3.6 and 3.7 the errors of both radius and angle are plotted, if λ is 10, 25 en 50.

$$\hat{\theta}_0 = \begin{bmatrix} 1 \\ 1 \\ 1 \end{bmatrix}$$

$$\Gamma^{-1} = \begin{bmatrix} 100 & 0 & 0 \\ 0 & 100 & 0 \\ 0 & 0 & 100 \end{bmatrix}$$

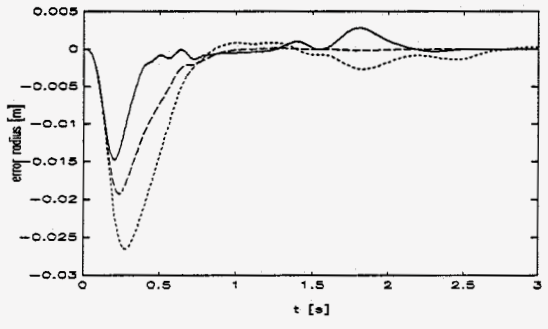

Figure B.1: 'error radius if λ is varied'
——: $\lambda=10$ --- : $\lambda=25$ ···: $\lambda=50$

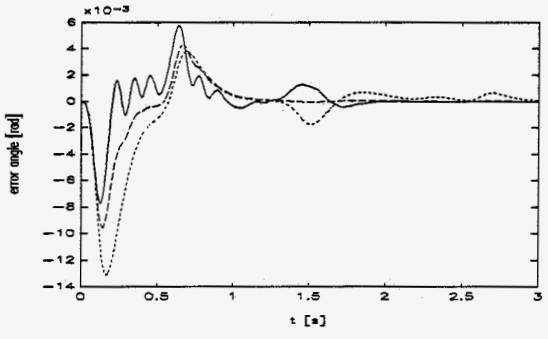

Figure B.2: 'error angle if λ is varied'
——: $\lambda=10$ --- : $\lambda=25$ ···: $\lambda=50$

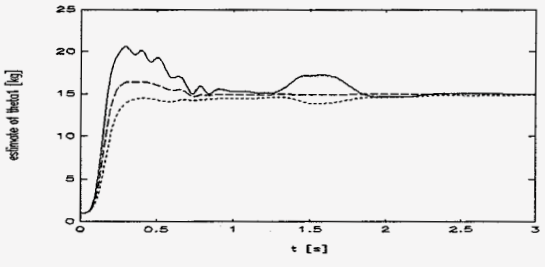

Figure B.3: 'estim. of θ_1'

—: $\lambda=10$ ---: $\lambda=25$ ···: $\lambda=50$

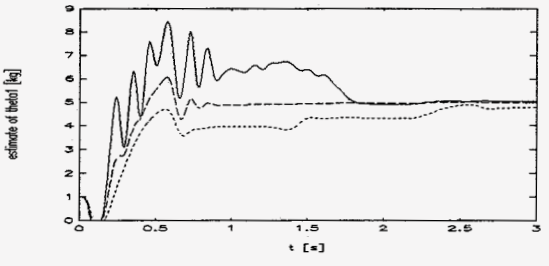

Figure B.4: 'estim. of θ_2'

—: $\lambda=10$ ---: $\lambda=25$ ···: $\lambda=50$

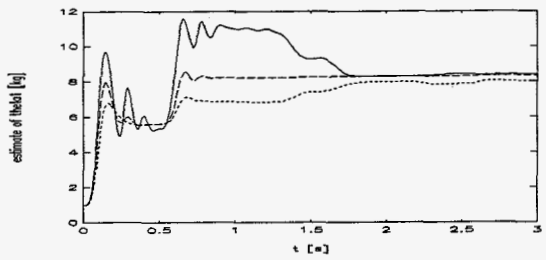

Figure B.5: 'estim. of θ_3'

——: $\lambda=10$ ---: $\lambda=25$ ···: $\lambda=50$

From these figures $\lambda=10$ was chosen to be the best. From this point all simulations were done with this value for λ. The adaptation proces has to be slower than the control proces. The adaptation gain matrix, chosen in paragraph 3.3, met that demand. So:

$$\Gamma^{-1} = \begin{bmatrix} 100 & 0 & 0 \\ 0 & 100 & 0 \\ 0 & 0 & 100 \end{bmatrix}$$

unless it is explicitly defined otherwise.

To determine the influence of the initial values, simulations are done where $\hat{\theta}_0$ is 0%, 50% en 75% of the true values.
In figures B.6 and B.7 the influence of the initial values on the errors are shown.

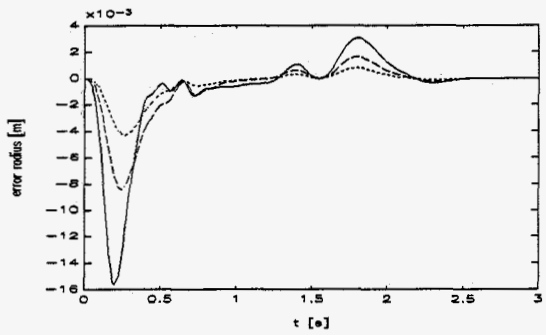

Figure B.6: 'error radius when varying θ_0'
——: θ_0=0% --- : θ_0=50% ···: θ_0=75%

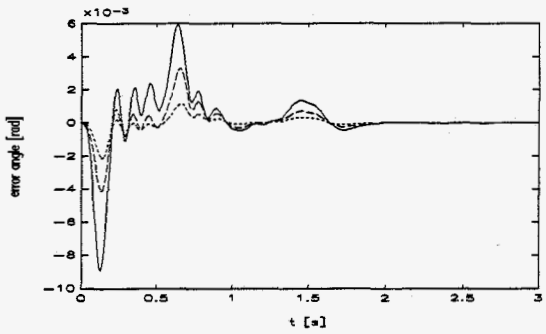

Figure B.7: 'error angle when varying θ_0'
——: θ_0=0% --- : θ_0=50% ···: θ_0=75%

In the figures below the estimated parameters are shown.

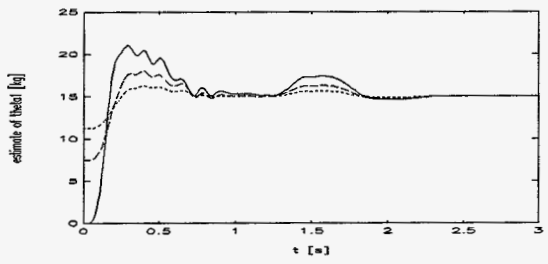

Figure B.8: 'estim. θ_1'
——:θ_0=0% ---:θ_0=50% ···:θ_0=75%

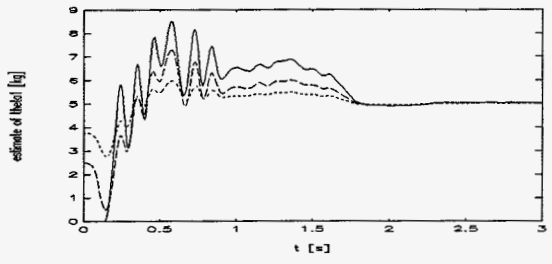

Figure B.9: 'estim. θ_2'
——:θ_0=0% ---:θ_0=50% ···:θ_0=75%

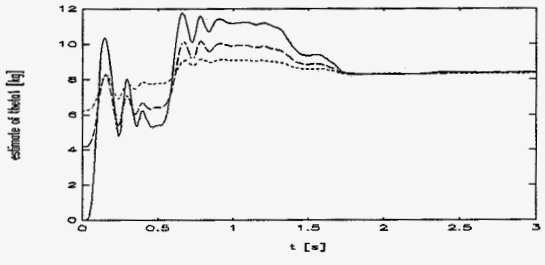

Figure B.10: 'estim. θ_3'
——:θ_0=0% ---:θ_0=50% ···:θ_0=75%

As could be expected the errors made are smaller when using a better initial estimate.

The influence of the adaptation gain matrix is plotted in figures B.11 and B.12.

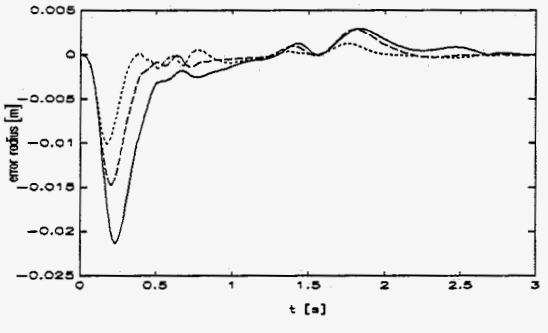

Figure B.11:'Radius error for varying Γ^{-1}'
——:Γ^{-1}=50I ---:Γ^{-1}=100I ···:Γ^{-1}=200I

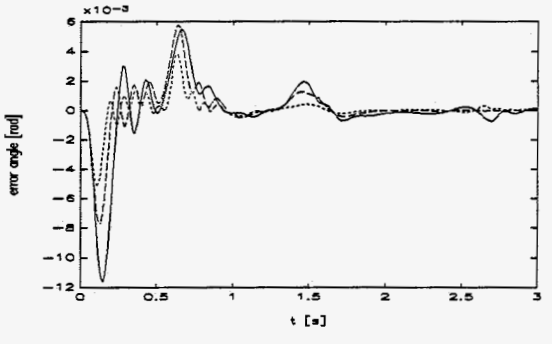

Figure B.12: 'Angle error when for Γ^{-1}'
——:Γ^{-1}=50I ---:Γ^{-1}=100I ···:Γ^{-1}=200I

The parameter estimates are plotted in figures B.13, B.14 and B.15 .

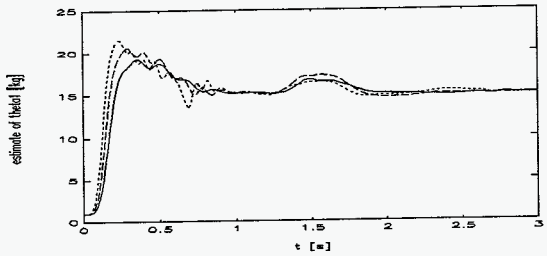

Figure B.13: 'estim. θ_1'

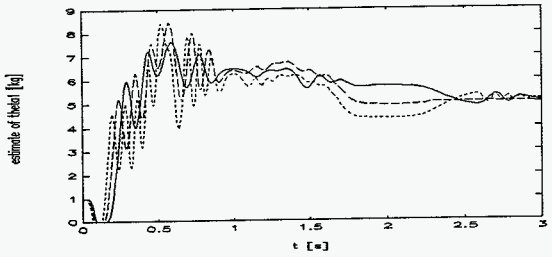

Figure B.14: 'estim. θ_2'

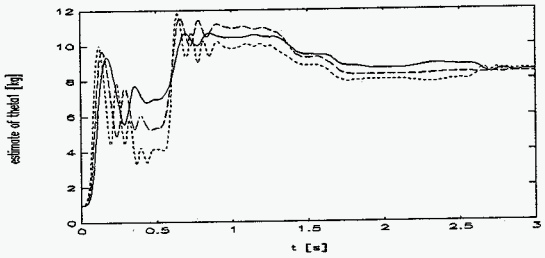

Figure B.15: 'estim. θ_3'

The estimations are faster but also more fluctuating when using a larger adaptation gain matrix. It seems that if $\Gamma^{-1}=200\ \mathbf{I}$ the errors are smaller than if Γ^{-1} is smaller.

B.2 Unmodelled dynamics

To compare the robustness of both controllers simulations are done with dynamics in the proces, which are not accounted for in the controller. These unmodelled dynamics are the result of dynamics of the servo motor.
With various values of λ the controller of R.Kelly gives us figures B.16 and B.17. The initial estimates are 0% of the exact values and $\Gamma^{-1} = \begin{bmatrix} 100 & 0 & 0 \\ 0 & 100 & 0 \\ 0 & 0 & 100 \end{bmatrix}$

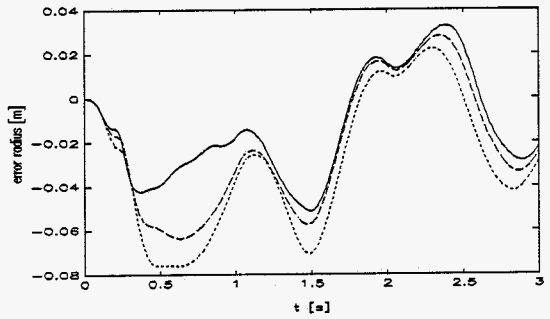

Figure B.16: 'Radius error for varying λ'
——: $\lambda=10$ --- : $\lambda=25$ ···: $\lambda=50$

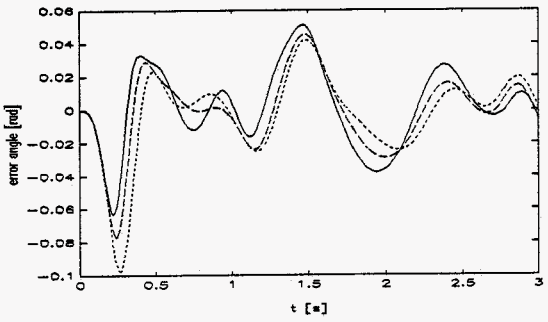

Figure B.17: 'Angle error for varying λ'
——: $\lambda=10$ --- : $\lambda=25$ ···: $\lambda=50$

In figures B.18, B.19 and B.20 the parameter estimates are plotted.

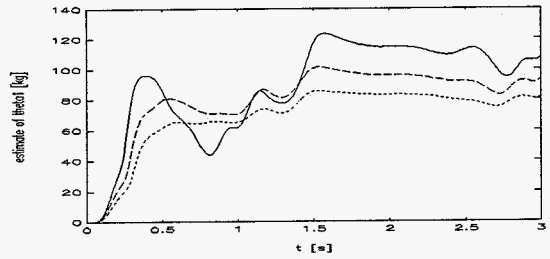

Figure B.18: 'estim. θ_1 for varying λ'
——:$\lambda=10$ ---:$\lambda=25$ ···:$\lambda=50$

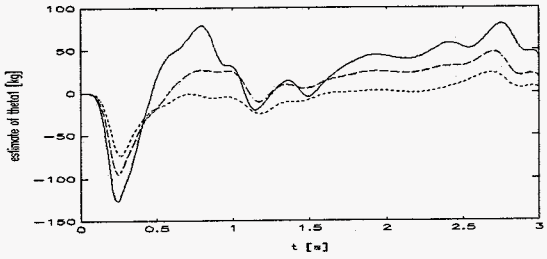

Figure B.19: 'estim. θ_2 for varying λ'
——:$\lambda=10$ ---:$\lambda=25$ ···:$\lambda=50$

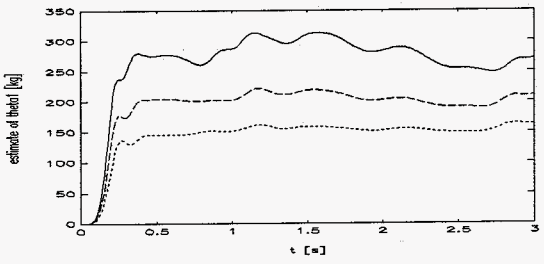

Figure B.20: 'estim. θ_3 for varying λ'
——:$\lambda=10$ ---:$\lambda=25$ ···:$\lambda=50$

We can conclude that $\lambda = 10$ is the optimal value of λ. From this point simulations, with unmodelled dynamics, are done with $\lambda = 10$. The adaptation gain matrix will be:

$$\Gamma^{-1} = \begin{bmatrix} 100 & 0 & 0 \\ 0 & 100 & 0 \\ 0 & 0 & 100 \end{bmatrix}.$$

As explaned in chapter 3, non-linear third order dynamics of the actuel system cause very high parameter estimates, when using a second order model in the controller

Now both controllers will be compared. The control parameters for the controller of Slotine-Li are the same as in paragraph 3.3. In these simulations the begin estimates are 0% of the real values.

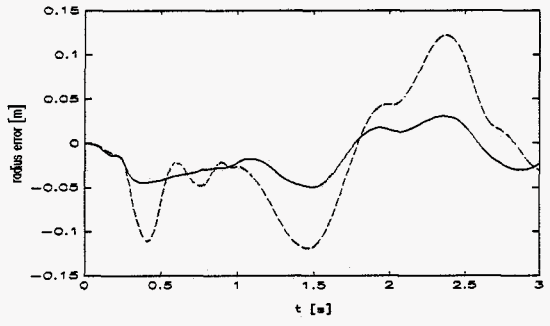

Figure B.21: 'error radius of both controllers'
——: R.kelly --- : Slotine-Li

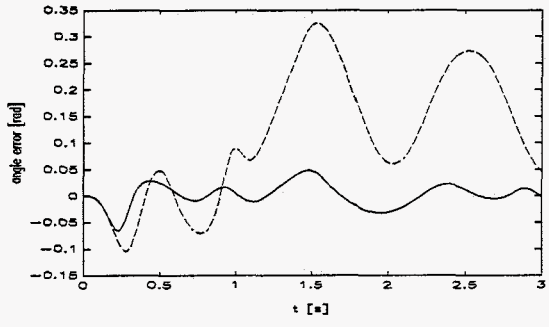

Figure B.22: 'error angle of both controllers'
——: R.Kelly --- : Slotine-Li

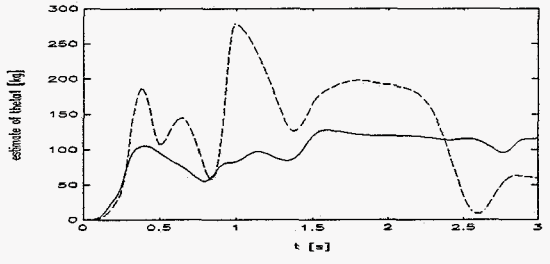

Figure B.23: 'estim. θ_1 against time'
——: R.Kelly --- : Slotine-Li

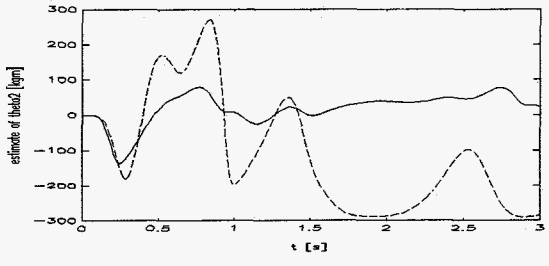

Figure B.24: 'estim. θ_2 against time'
——: R.Kelly --- : Slotine-Li

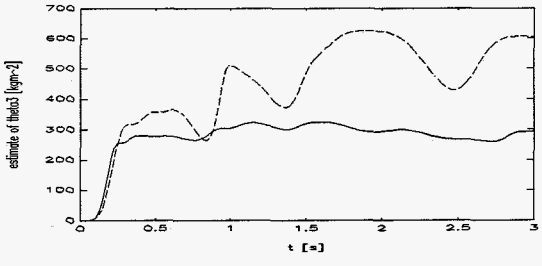

Figure B.25: 'estim. θ_3 against time'
——: R.Kelly --- : Slotine-Li

The behaviour of the controllers doesn't change much if we use as begin estimate 0% or 100% of the exact value. Because in both cases the parameters converge to values, which are orders higher than the exact values, the influence of an initial value between 0% and 100% is minimal.
The system is a non-linear third order system, which is modelled in the controller by a second order model. This results in much larger values of the parameter estimates. The non-linearity of the actual system causes remaining errors. This is why the estimates don't converge.

B.3 Friction

In this paragraph simulations are shown where unmodelled dynamics as well as friction are used. Up till now the bar with load could be pushed up and down by force F(t) without resistance.In the following simulations friction is introduced, as defined in subparagraph 3.4.3.
The friction parameters are:

- θ_4 = 10 [N] : parameter of coulomb friction.
- θ_5 = 5 [Ns/m] : parameter of viscous friction.

The control parameters during the simulations with friction were:

$$\Gamma^{-1} = \begin{bmatrix} 100 & 0 & 0 & 0 & 0 \\ 0 & 100 & 0 & 0 & 0 \\ 0 & 0 & 100 & 0 & 0 \\ 0 & 0 & 0 & 50 & 0 \\ 0 & 0 & 0 & 0 & 50 \end{bmatrix}$$

$$\lambda = 10$$

The adaptation gains of the friction parameters were chosen as in L.J.W. van Gerwen [4].

The following figures show us the results of these simulations.

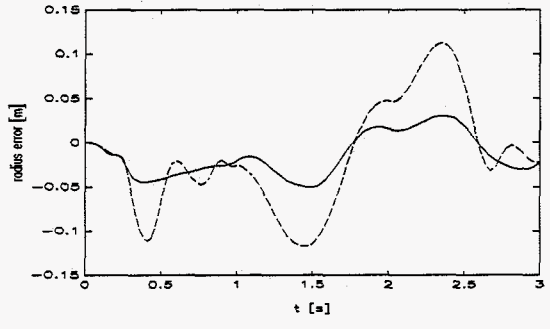

Figure B.26: 'error radius of both controllers'
—— : R.Kelly --- : Slotine-Li

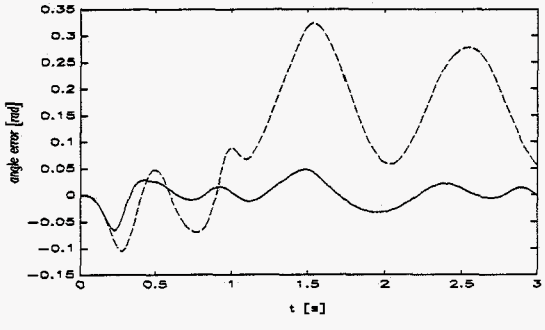

Figure B.27: 'error angle of both controllers'
—— : R.Kelly --- : Slotine-Li

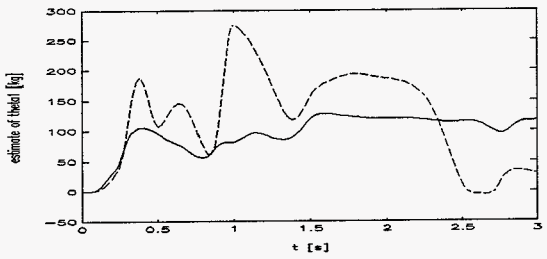

Figure B.28: 'estimate θ_1 against time'
——— : R.Kelly --- : Slotine-Li

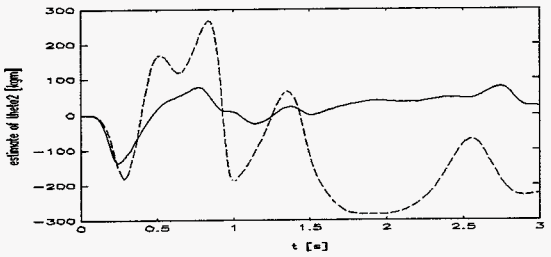

Figure B.29: 'estimate θ_2'
——— : R.Kelly --- : Slotine-Li

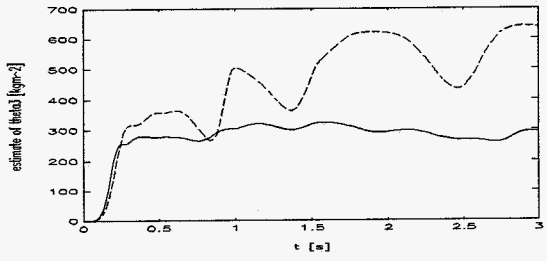

Figure B.30: 'estimate θ_3'
——— : R.Kelly --- : Slotine-Li

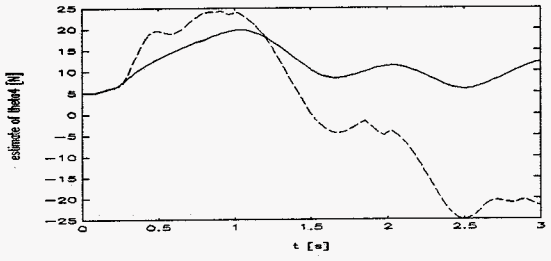

Figure B.31: 'estimate θ_4'
——— : R.Kelly --- : Slotine-Li

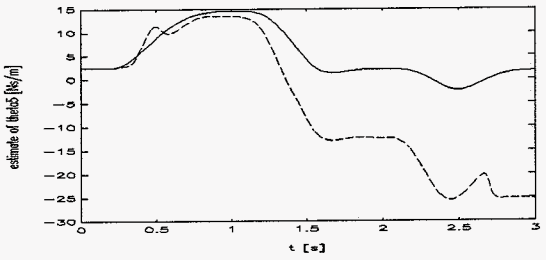

Figure B.32: 'estimate θ_5'
——— : R.Kelly --- : Slotine-Li

From the simulations above it can be seen that the influence of friction on the control behaviour is small compared to the influence of the motor dynamics.

Appendix C:

Model of the XY-table

In the appendix the equations of motion are presented, which also can be found in L.J.W. van Gerwen [4]. Below figure 4.2 is shown again.

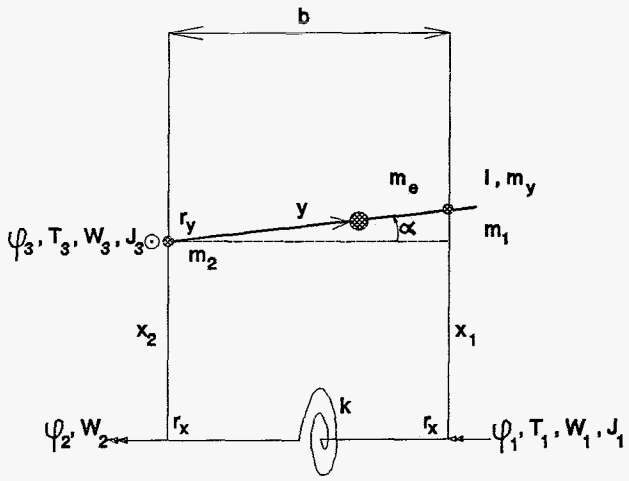

Figure 4.2: 'Simulated system'

The used symbols of the figure above are:

φ_1	angular displacement of belt wheel 1
φ_2	angular displacement of belt wheel 2
φ_3	angular displacement of belt wheel 3
x_1	position of x-slide 1 on slideway 1
x_2	position of x-slide 2 on slideway 2
y	position of end-effector on y-slideway
b	distance between slideway 1 and slideway 2
l	length of y-slideway
r_x	radius of the belt wheels 1 and 2
r_y	radius of the belt wheel 3
m_1	mass of x-slide 1
m_2	mass of x-slide 2
m_y	mass of y-slideway including the motor
m_e	mass of end-effector
J_1	moment of inertia associated with φ_1
J_2	moment of inertia associated with φ_2 (assumed to be zero)
J_3	moment of inertia associated with φ_3
W_1	friction torque associated with φ_1
W_2	friction torque associated with φ_2
W_3	friction torque associated with φ_3
T_1	motor torque on belt wheel 1
T_3	motor torque on belt wheel 3
k	torsion spring constant

Now x_1, x_2 and y can be written as follows:

$$\begin{aligned} x_1 &= r_x \varphi_1 \\ x_2 &= r_x \varphi_2 \\ y &= r_y \varphi_3 \end{aligned}$$

and α is defined as:

$$\alpha = \arctan\left(\frac{x_1 - x_2}{b}\right)$$

All masses are considered to be point masses and α is assumed to be small, so:

$$\alpha \simeq \left(\frac{x_1 - x_2}{b}\right) \qquad ; \cos(\alpha) \simeq 1 \qquad ; \sin(\alpha) \simeq \alpha$$

As mentioned in L.J.W. van Gerwen the equations of motion are derived with the help of the method of Lagrange and the software package MAPLE. This resulted in:

$$M(q)\ddot{q} + h(q,\dot{q}) = f \tag{C.1}$$

with:

$$q^T = [\varphi_1 \;\; \varphi_2 \;\; \varphi_3]$$

$$M_{11} = J_1 + \left[m_1 + \tfrac{1}{3}m_y\left(\frac{l}{b}\right)^2 + m_e\left(\frac{r_y\varphi_3}{b}\right)^2\right] r_x^2$$

$$M_{12} = M_{21} = \left[\tfrac{1}{2}m_y\left(\frac{l}{b}\right) - \tfrac{1}{3}m_y\left(\frac{l}{b}\right)^2 + m_e\left(\frac{r_y\varphi_3}{b}\right) - m_e\left(\frac{r_y\varphi_3}{b}\right)^2\right] r_x^2$$

$$M_{13} = M_{31} = 0$$

$$M_{22} = \left[m_2 + m_y - m_y\left(\frac{l}{b}\right) + \tfrac{1}{3}m_y\left(\frac{l}{b}\right)^2 + m_e - 2m_e\left(\frac{r_y\varphi_3}{b}\right) + m_e\left(\frac{r_y\varphi_3}{b}\right)^2\right] r_x^2$$

$$M_{23} = M_{32} = \left(m_e\frac{(\varphi_1 - \varphi_2)r_y}{b}\right) r_x^2$$

$$M_{33} = J_3 + m_e r_y^2$$

$$h_1 = 2m_e r_y \varphi_3 \frac{r_y r_x^2}{b^2}(\dot{\varphi}_1 - \dot{\varphi}_2)\dot{\varphi}_3 + k(\varphi_1 - \varphi_2)$$

$$h_2 = 2m_e(b - r_y\varphi_3)\frac{r_y r_x^2}{b^2}(\dot{\varphi}_1 - \dot{\varphi}_2)\dot{\varphi}_3 - k(\varphi_1 - \varphi_2)$$

$$h_3 = -m_e r_y \varphi_3 \frac{r_y r_x^2}{b^2}(\dot{\varphi}_1 - \dot{\varphi}_2)^2$$

$$f_1 = T_1 - W_1 \operatorname{sign}(\dot{\varphi}_1)$$

$$f_2 = -W_2 \operatorname{sign}(\dot{\varphi}_2)$$

$$f_3 = T_3 - W_3 \operatorname{sign}(\dot{\varphi}_3)$$

Equations C.1 are used in chapter 4 to simulate the XY-table. The model used for the controllers is simplified by assuming that there is no torsion spring. In this case the angles φ_1 and φ_2 are the same. This results in:

$$M(q)\ddot{q} + w(q,\dot{q}) = \tau \tag{C.2}$$

with:

$$
\begin{aligned}
q^T &= [\varphi_1 \quad \varphi_3] \\
M_{11} &= J_1 + [m_1 + m_2 + m_e + m_y]\, r_x^2 \\
M_{12} &= M_{21} = 0 \\
M_{22} &= J_3 + m_e r_y^2 \\
w_1 &= (W_1 + W_2)\, \mathrm{sign}(\dot{\varphi}_1) \\
w_2 &= W_3\, \mathrm{sign}(\dot{\varphi}_3) \\
\tau_1 &= T_1 \\
\tau_2 &= T_2
\end{aligned}
$$

Appendix D:

System and controller matrices for the XY-table

The matrices of equation 2.1 in case of the XY-table are:

$$H = \begin{bmatrix} \theta_1 & 0 \\ 0 & \theta_2 \end{bmatrix} \qquad C = \begin{bmatrix} 0 & 0 \\ 0 & 0 \end{bmatrix}$$

$$g = \begin{bmatrix} 0 \\ 0 \end{bmatrix} \qquad q = \begin{bmatrix} \varphi_1 \\ \varphi_3 \end{bmatrix}$$

$$\tau = \begin{bmatrix} T_1 \\ T_2 \end{bmatrix} \qquad v = \begin{bmatrix} v_1 \\ v_2 \end{bmatrix}$$

In case of the controller of R.Kelly, the matrix Φ from equation 2.4 can be written as:

$$\Phi = \begin{bmatrix} \ddot{\varphi}_{1_d} + K_{v_1}\dot{\varphi}_{1_e} + K_{p_1}\varphi_{1_e} & 0 & -\text{sign}(\dot{\varphi}_1) & 0 \\ 0 & \dot{\varphi}_{3_d} + K_{v_2}\dot{\varphi}_{3_e} + K_{p_2}\varphi_{1_e} & 0 & -\text{sign}(\dot{\varphi}_3) \end{bmatrix}$$

In case of Slotine-Li, the matrix Y is:

$$Y = \begin{bmatrix} \ddot{\varphi}_{1_r} & 0 & -\text{sign}(\dot{\varphi}_1) & 0 \\ 0 & \ddot{\varphi}_{3_r} & 0 & -\text{sign}(\dot{\varphi}_3) \end{bmatrix}$$

Appendix E:

Estimation of control parameter λ_i when simulating a controlled XY-table

In paragraph 4.2 the control matrices K_v and K_p, for the controller of R.Kelly, were determined. To simulate an XY-table, controlled by R.Kelly, there is one parameter yet to be determined, i.e. λ. This is done by simulating the system with several values of λ. In the following figures the errors, in x- and y-direction, are shown.

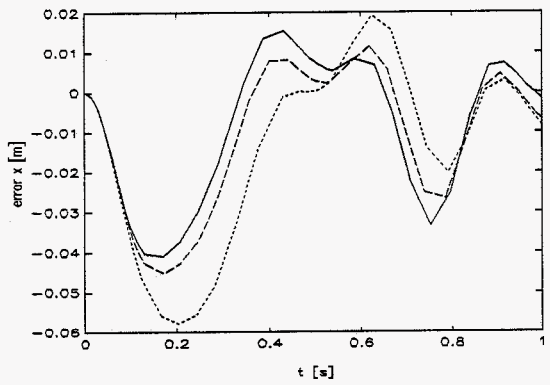

Figure E.1: 'Error in x-direction'
——— : 'λ=5 --- : λ=10 ··· : λ=25

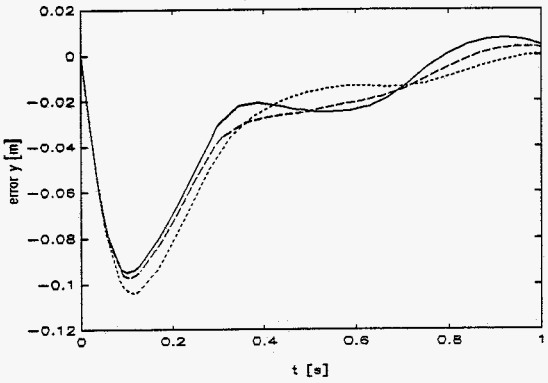

Figure E.2: 'Error in y-direction'
——— : λ=5 --- : λ=10 ··· : λ=25

From these figures, $\lambda = 10$ was chosen to be the optimal value.

Appendix F:

Design of Kalman observer

The kalman observer was chosen the same as the kalman observer designed by L.J.W. van Gerwen [4]. We use the simplified model described by equations 5.1 and 5.2.

$$\theta_1 \ddot{x} = F_1 - \theta_3 \, \text{sign}(\dot{x}) \tag{5.1}$$

$$\theta_2 \ddot{y} = F_2 - \theta_4 \, \text{sign}(\dot{y}) \tag{5.2}$$

When state, input and output in x-direction are defined by:

state: $x(t) = \begin{bmatrix} x(t) \\ \dot{x}(t) \end{bmatrix}$

input: $u(t) = F_1$

output: $y(t) = x(t)$

the time discrete model can be written as:

$$x(n+1) = A_d x(n) + B_d [u(n) - P_2 \, \text{sign}(\dot{x}(n))] + G_d w(n) \tag{F.1}$$

$$y(n) = C_d x(n) + v(n) \tag{F.2}$$

, where w(n) is the discrete process noise and $v(n)$ is the discrete measurement noise.
If T_s is the sampling time, then the matrices of E.1 and E.2 can be written as follows:

$$A_d = \begin{bmatrix} 1 & T_s \\ 0 & 1 \end{bmatrix} \; ; \; B_d = G_d = \frac{1}{P_1} \begin{bmatrix} T_s^2 \\ T_s \end{bmatrix} \; ; \; C_d = \begin{bmatrix} 1 & 0 \end{bmatrix}$$

According to equation (6.54) of Kok [5] an estimate can be made one sample ahead:

$$\hat{x}(n+1) = A_d \hat{x}(n) + B_d [u(n) - P_2 \, \text{sign}(\dot{x}(n))] + K(y(n) - C_d \hat{x}(n)) \tag{F.3}$$

with the optimal gain matrix K^0 according to equation (6.69) of Kok [5]:

$$K^0 = A_d \tilde{Q} C_d^T [V_v + C_d \tilde{Q} C_d^T]^{-1} \tag{F.4}$$

Because there are no significant changes in the covariances, the same values were used during the experiments as found in L.J.W. van Gerwen:

$$K_x^o = A_d \cdot \begin{bmatrix} 1 \\ 207 \end{bmatrix}$$

$$K_y^o = A_d \cdot \begin{bmatrix} 0.6 \\ 140 \end{bmatrix}$$

Appendix G:

Estimation of control parameter λ of R.Kelly, when experimenting with the XY-table

Before both controllers can be compared, λ has to be determined first. For this purpose some experiments were done with several different values of λ. After that the optimal value of λ was determined with the following minimization criterium:

$$J_e = \sum_{i=1}^{n} e_i^T W e_i$$

with:

- J_e = minimization functional
- W = wheighing matrix
- e = column with errors in x- and y-direction
- n = number of measurements

To exclude errors made by the difference in begin position, measurements were taken from t=2 sec. The matrix W was taken to be the unity matrix, so the errors made in both directions are wheighed equally.
In the figures below the errors are shown, in case of the diagonal as the desired trajectory.

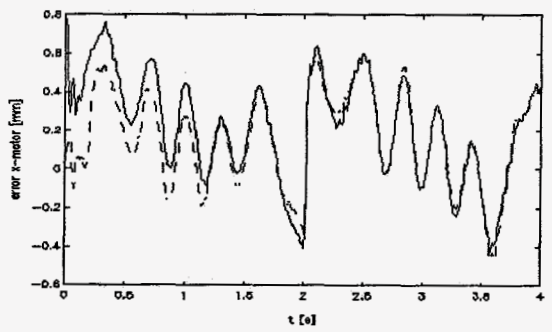

Figure G.1: 'Error x-motor'
——: λ=10 --- : λ=20

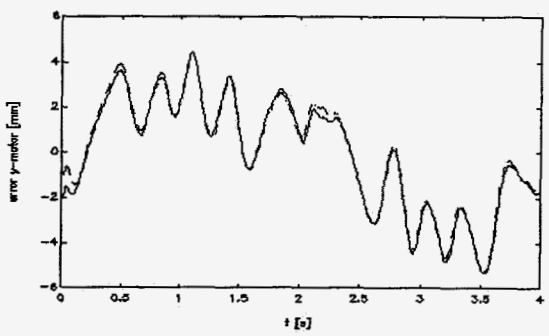

Figure G.2: 'Error y-motor'
——: λ=10 --- : λ=20

After minimizing the functional J_e the optimal value of λ was found to be λ=20.

When using the circle as the desired trajectory, the following plots were obtained:

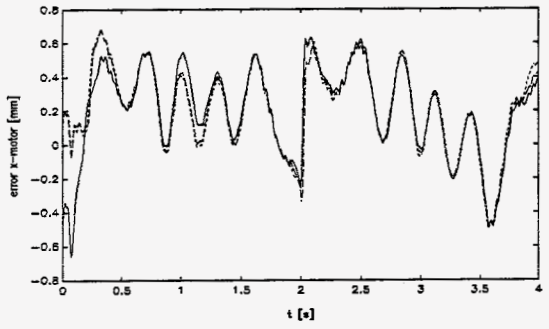

Figure E.3: 'Error x-motor'
——: $\lambda=5$ --- : $\lambda=10$ ···: $\lambda=20$

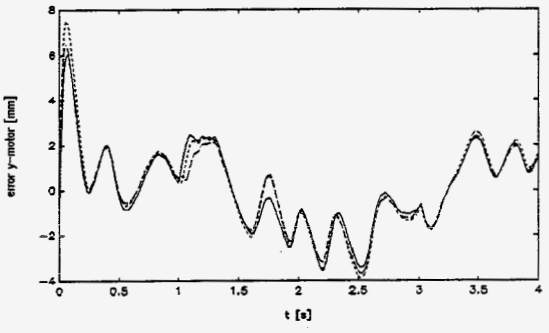

Figure E.4: 'Error y-motor'
——: $\lambda=5$ --- : $\lambda=10$ ···: $\lambda=20$

After minimizing the functional J_e $\lambda=5$ was found to be the optimal value.

Appendix H:

Experiment results of the XY-table

In this appendix results are shown, which are not nessecary to understand the report, but give a better insight in the behaviour of the two controllers.

Additional to the experiments shown in chapter 5, experiments with a worse initial estimate were done. In the experiments below initial estimates of 25% were used. During the experiments two trajectories were used:

- the straight line (diagonal)
- the circle

In case of the rigid system and the diagonal trajectory the following errors and estimates could be obtained:

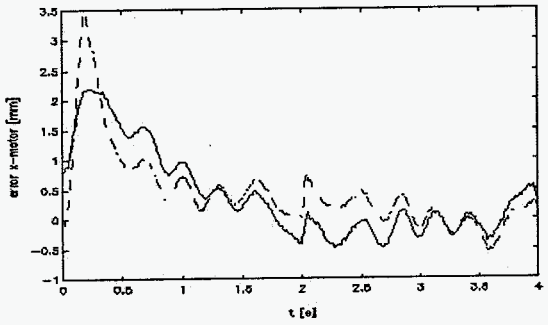

Figure H.1: 'Error x-motor'
——: Slotine-Li --- : R.Kelly

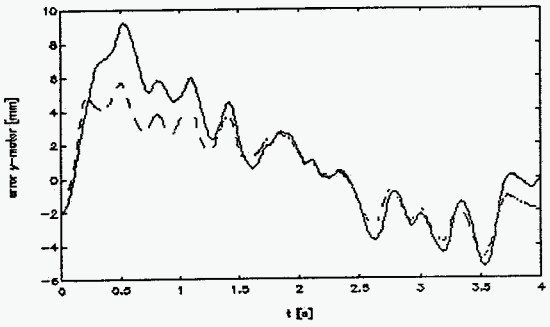

Figure H.2: 'Error y-motor'
——; Slotine-Li --- : R.Kelly

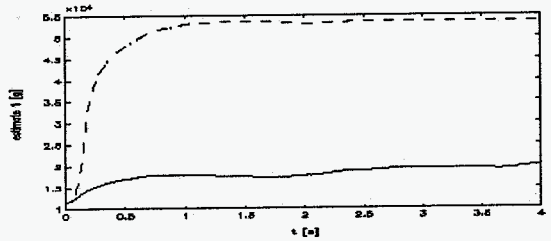

Figure H.3: 'Estimate θ_1'
——: Slotine-Li --- : R.Kelly

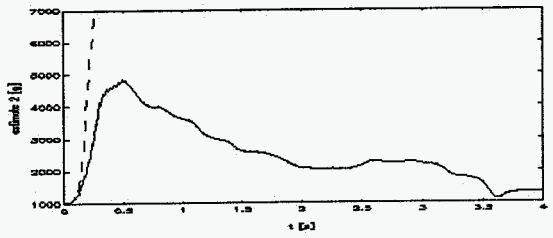

Figure H.4: 'Estimate θ_2'
——: Slotine-Li --- : R.Kelly

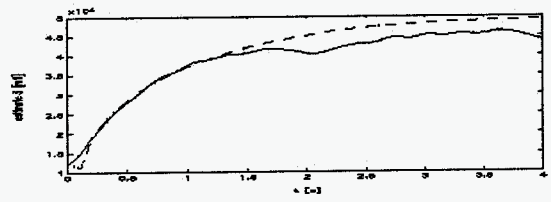

Figure H.5: 'Estimate θ_3'
——: Slotine-Li --- : R.Kelly

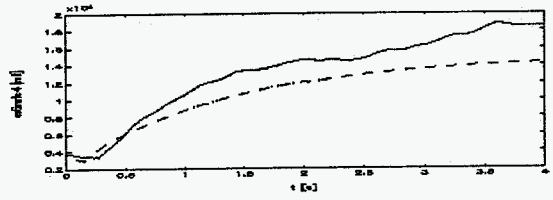

Figure H.6: 'Estimate θ_4'
——: Slotine-Li --- : R.Kelly

The controller of R.Kelly performs better, especially in y-direction. The reason can be found in the better estimation of the parameters. A reason for the better estimation, could be the influence of speed errors on the adaptation proces. In the linearity matrix *Y*, in case of Slotine-Li, only the desired acceleration and the error in the speed is present. Errors in the speed estimation have greater influence on the estimation of the parameters, in case of Slotine-Li, than in case of R.Kelly.
In the figures of the estimates the more fluctuating behaviour of the estimations of Slotine-Li is very clear.

When using the circle as desired trajectory the figures below were obtained.

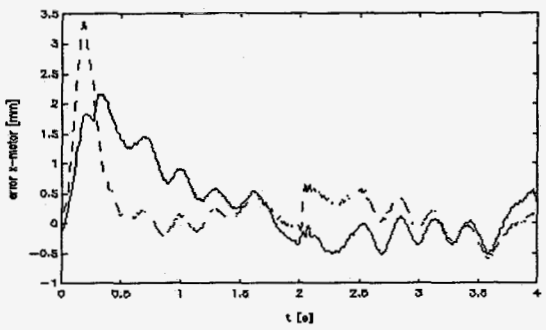

Figure H.7: 'Error x-motor'
——: Slotine-Li --- :R.Kelly

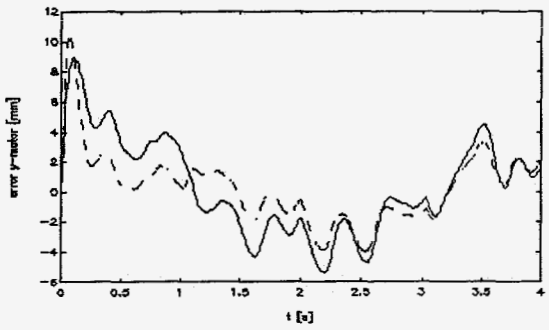

Figure H.8: 'Error y-motor'
——: Slotine-Li --- : R.Kelly

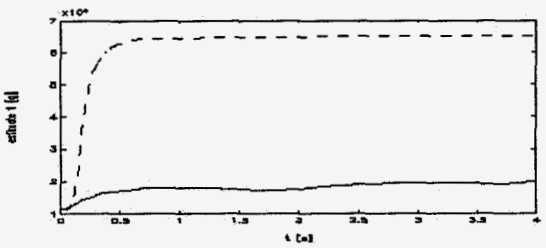

Figure H.9: 'Estimate θ_1'
——: Slotine-Li --- : R.Kelly

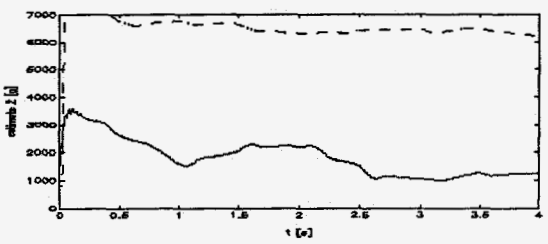

Figure H.10: 'Estimate θ_2'
——: Slotine-Li --- : R.Kelly

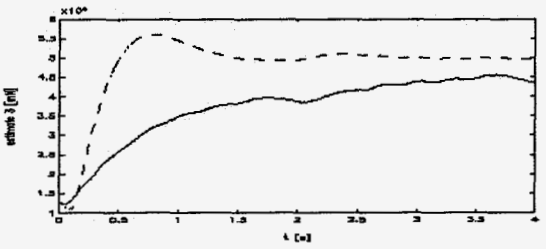

Figure H.11: 'Estimate θ_3'
——: Slotine-Li --- : R.Kelly

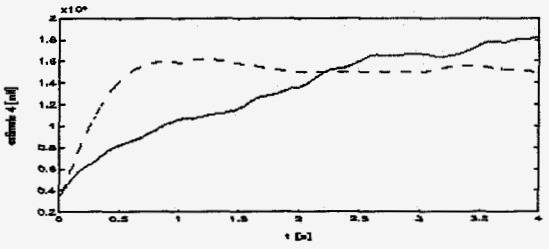

Figure H.12: 'Estimate θ_4'
——: Slotine-Li --- : R.Kelly

Here too the less fluctuating behaviour of the estimates, made by the controller of R.Kelly, is very clearly. The smaller errors, made by Slotine-Li, around 0.25 sec. can be found in the higher PD-feedback at that moment. The reason for this is the fact that the PD-feedback of Slotine-Li has terms with the estimated parameters but also terms without the estimated parameters. The controller of R.Kelly, however, has only feedback terms with the estimated parameters, which result in a low gain, when the initial parameter estimates are small.

References

[1] **Kelly, R.**
Adaptive computed torque plus compensation control for robot manipulators
Mech. Mach. Theory, Vol. 25, No. 2, 1990

[2] **Slotine, J.J.E. and W. Li**
Adaptive manipulator control: A case study
I.E.E.E Int. Conf. Robotics and Automation, Vol. 3, 1987

[3] **Freund, E**
Fast nonlinear control with arbitrary pole-placement for industrial robots
Int. Jnl. of Robotics Research, Vol.1, No.1, 1982

[4] **Gerwen, L.J.W. van**
An adaptive robot controller: Design, simulation and implementation
Report WFW 90.036, Dep. of Mechanical Engineering, University of Tecnology, Eindhoven, 1990

[5] **Kok, J.J.**
Werktuigkundig regelen 2
Lecture notes 4594, Dep. of Mechanical Engineering, University of Technology, Eindhoven, 1985